JOURNAL OF GEOPHYSICAL RESEARCH, VOL. 106, NO. C5, PAGES 9473–9497, MAY 15, 2001

Optics, particles, stratification, and storms on the New England continental shelf

W. D. Gardner,[1] J. C. Blakey,[1] I. D. Walsh,[1,2] M. J. Richardson,[1] S. Pegau,[3]
J. R. V. Zaneveld,[3] C. Roesler,[4] M. C. Gregg,[5] J. A. MacKinnon,[5]
H. M. Sosik,[6] and A. J. Williams III[6]

Abstract. In situ beam attenuation and chlorophyll fluorescence were correlated with concentration and bulk composition of particles in shelf waters during summer and spring under different physical forcing conditions to determine if optical parameters could be used as an additional tracer in examining the process of mixing in shelf waters. Time series measurements were made for two 18 day periods during high stratification (late summer 1996, $\Delta\sigma_t$ = ~3.0 kg m^{-3} surface to bottom) and low but rapidly developing stratification (spring 1997, $\Delta\sigma_t$ = 0.05 to 0.5 kg m^{-3}) in 70 m of water in a midshelf environment south of Martha's Vineyard, Massachusetts. When defined by hydrography and optical profiles, four layers were identified during the summer: the surface mixed layer, the particle/chlorophyll maximum, the midwater particle minimum, and the bottom nepheloid layer. Fast moving solitons perturbed the water column briefly, but no storms perturbed the system until large surface swells from Hurricane Edouard intensified and thickened the nepheloid layer. Bulk composition and optics of particles in and above the nepheloid layer were distinctly different after the passage of Hurricane Edouard. The hurricane passage demonstrated that intense atmospheric forcing greatly influences both hydrographic and optical properties in the entire water column, even when highly stratified ($\Delta\sigma_t$ = ~3.0 kg m^{-3}, decreasing to 0.8 kg m^{-3} post hurricane), and causes massive resuspension, due initially to wave shear stress that was later dominated by current shear. Restratification progressed rapidly after the hurricane passed. During spring the water column started as a weakly stratified two-layer system hydrographically and optically but evolved into three layers as stratification developed. Strong spring storms affected both surface and bottom layers but with decreasing impact as the water column stratified.

1. Introduction

1.1. Background and Objectives

Continental shelves are regions of intense physical forcing, so shelf water characteristics may undergo dramatic changes over both short- and long-term timescales. In temperate climates, shelf waters experience annual cycles of winter cooling, mixing, and minimal stratification followed by spring and summer heating, resulting in strong stratification [*Loder and Greenberg*, 1986]. On shorter timescales the vertical structure of the water column can be affected by winds, waves, tides, internal waves and solitons, intrusions of slope water, and storm events [*Orr et al.*, 2000; *Sandstrom and Elliott*, 1984; *Haury et al.*, 1983; *Chang and Dickey*, this issue]. The stratification and mixing of the water column affects particulate matter distributions and concentrations. For example, atmospheric forcing can mix the surface boundary layer, moving particles downward [*Gardner et al.*, 1995]. Intense bottom boundary layer mixing and sediment resuspension can result from tidal forcing, currents, and long-period waves [*Butman*, 1987]. Stratification in spring can lead to plankton blooms, which increase the concentration of biogenic particles within the water column [*Platt et al.*, 1991; *Sosik et al.*, this issue]. During periods of high stratification, particles are constrained to the portion of the water column in which they were generated unless they are consumed, remineralized, or settle to lower regions. Strong stratification inhibits mixing across isopycnals, whereas mixing is more likely to occur in weakly stratified waters.

To improve understanding of mixing processes and their influence on ocean optics and particle distributions in the coastal ocean, the Coastal Mixing and Optics experiment (CMO) was initiated [*Dickey and Williams*, this issue]. The overall objective of CMO was to examine vertical mixing processes associated with the seasonal pycnocline and boundary layers (surface and bottom) and their influence on hydrographic structure and distribution of optical properties of particulate and dissolved matter.

The CMO objectives of this paper are to (1) characterize and compare hydrographic and optical structures during periods of

[1]Department of Oceanography, Texas A&M University, College Station, Texas.
[2]Now at College of Oceanic and Atmospheric Sciences, Oregon State University, Corvallis, Oregon.
[3]College of Oceanic and Atmospheric Sciences, Oregon State University, Corvallis, Oregon.
[4]Bigelow Laboratory for Ocean Sciences, West Boothbay Harbor, Maine.
[5]Applied Physics Laboratory and School of Oceanography, University of Washington, Seattle, Washington.
[6]Woods Hole Oceanographic Institution, Woods Hole, Massachusetts.

Paper number 2000JC900161.
0148-0227/01/2000JC900161$09.00

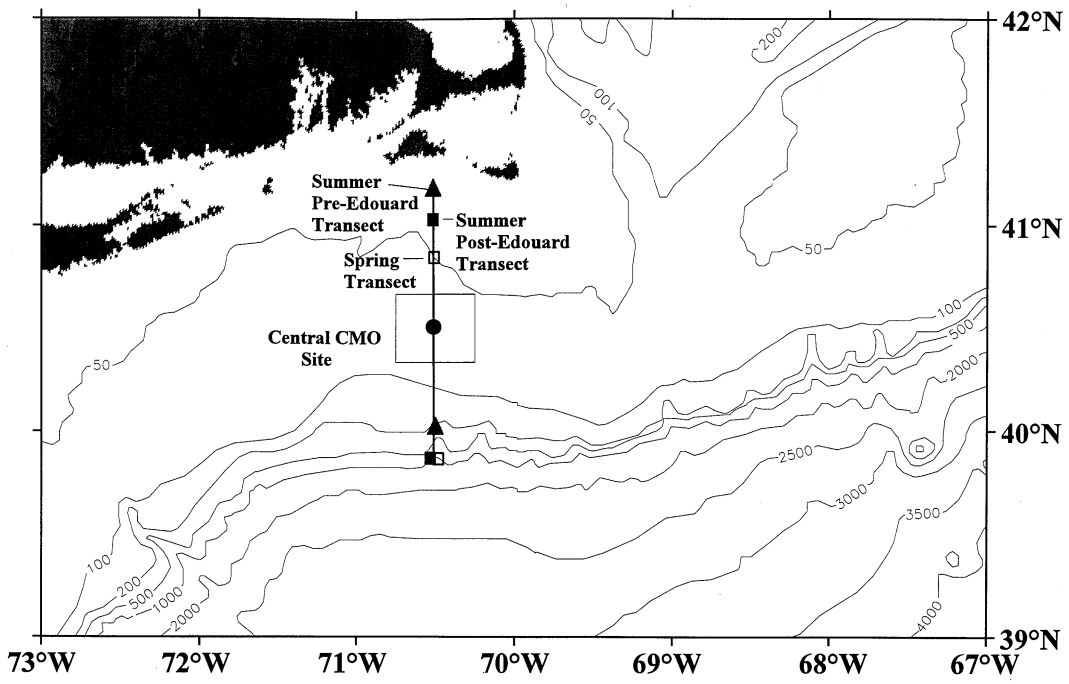

Figure 1. Map of CMO study area. The symbols mark the endpoints of transects made at the beginning of the summer cruise (triangles, August 17-18, 1996; Plate 1), the post-Hurricane Edouard transect (solid squares, September 5-7, 1996; Plate 2), and the end of the spring cruise (open squares, May 12-13, 1997; Plate 5). Time series measurements were made within the circle at the central CMO site.

high (summer) and low (spring) stratification on the midshelf, (2) determine the bulk particle properties throughout the water column to characterize particles as biogenic or terrigenous in different seasons, (3) compare the bulk particle properties (concentration, organic carbon, and chlorophyll) with optical parameters of beam attenuation and chlorophyll fluorescence to characterize further water "masses" or layers, and (4) determine how optical and bulk composition and distribution of particles change with different seasons, stratification, and forcing functions (storms, currents, waves, etc.).

1.2. Study Area

The CMO study area was located on the continental shelf south of Martha's Vineyard, Massachusetts, between 70° and 71°W, 40°15' and 40°45'N (Figure 1) in a region known as the "Mud Patch," which is the only region on the eastern seaboard that contains >30% silt in bottom sediments [*Twitchell et al.*, 1981]. This area was chosen because of its location seaward of the coastal boundary layer, distance landward from the shelf break front, distance from riverine sources of dissolved and particulate matter and freshwater buoyancy effects, smooth bottom topography, lack of major geostrophic currents, considerable historical knowledge about the area's seasonal hydrography, presence of fine-grained bottom sediment for resuspension, and proximity to ports with research ships. Our time series station was located in the middle of the study area at approximately 70°30'W, 40°30'N in 70 m of water.

Historical data from this region suggest that along-shelf currents range from 5 to 15 cm s^{-1} and dominate slightly over the cross-shelf component, which is 5 to 10 cm s^{-1}. The average tidal component is 6-14 cm s^{-1} [*Manheim et al.*, 1970; *Butman et al.*, 1979; *Moody et al.*, 1987]. Surface currents are generally southwestward at speeds of 20 cm s^{-1} [*Mayer et al.*, 1979]. Average bottom currents have been measured at 3.2 cm s^{-1} in a west to southwest direction [*Bumpus and Lauzier*, 1965; *Butman et al.*, 1982]. Winter storms can generate current speeds of up to 45 cm s^{-1} with water displacements of up to 100 km during a single event [*Beardsley and Butman*, 1974; *Butman and Nobel*, 1978]. The currents for CMO are described by *Chang et al.* [this issue].

The region is known for strong seasonal changes in hydrography. *Flagg* [1987] describes the primary water masses in the area as Georges Bank Water (summer to winter temperatures and salinity ranging from 16° to 3°C and 32.2 to 33.0 psu, respectively) and Maine Surface Water (ranging from 17° to 1°C and 33.2 to 31.6 psu). In late fall the surface layer cools, sinks, and mixes until the entire water column is nearly homogeneous [*Houghton et al.*, 1982; *Palanques and Biscaye*, 1992]. During the winter a "cold pool" of water develops at the 60-70 m isobaths [*Houghton et al.*, 1982]. Toward late spring, the surface waters are heated by solar radiation and increase in stratification so the water column is strongly stratified by midsummer, trapping the cold pool at depth. A shelf slope front is also commonly found south of our CMO time series station [*Ryan et al.*, 1999]. The 1 year time series of hydrographic conditions for this experiment is presented by *Chang and Dickey* [this issue].

The shelf water column generally consists of three hydrodynamic zones: the surface and bottom boundary layers and the region between the boundary layers, including the pycnocline. The boundary layers merge in the inner coastal zone, eliminating the middle zone. The surface layer is mixed by winds and stratified by solar heating [*Price and Weller*, 1986] and can be defined as the depth at which σ_t has changed by a fixed amount [*Brainerd and Gregg*, 1995] ($\Delta \sigma_t = 0.01$ in this study). The mixed layer depth (MLD) ranges from a few meters during

summer to tens of meters in winter. The bottom boundary layer or bottom mixed layer is affected by drag forces as water moves along the bottom or is mixed by wave energy penetrating to the seafloor [*Butman*, 1987].

The distribution of particles in the water column depends on (1) biological processes that form and destroy particles: primary and secondary production, respiration, and remineralization; (2) physical processes that introduce particles: advection from riverine sources and resuspension of bottom sediments; and (3) physical and biological processes that redistribute particles: mixing, advection, aggregation/disaggregation, biological packaging, and sinking. As a result, particles in surface waters away from rivers are usually dominated by biological material, and particles in bottom waters are dominated by resuspended sediments and detritus settled from surface waters [*Meade* et al., 1975]. Primary production is much higher on the shelf than in the open ocean because of nutrient input from rivers, coastal upwelling, and deep winter mixing. Particulate matter (PM) concentrations measured in surface waters of the CMO area have been between 0.5 and 3.0 mg L^{-1}, with up to 65% being combustible organic matter [*Manheim et al.*, 1970; *Meade et al.*, 1975; *Bothner et al.*, 1981]. Combustible particulate organic matter is usually <30% in bottom waters. PM concentrations as great as 15 mg L^{-1} have been measured in bottom waters following winter storms [*Bothner et al.*, 1981].

A bottom mixed layer can be identified as a zone of constant temperature or density [*Armi and D'Asaro*, 1980] and is often associated with a nepheloid layer whose thickness may or may not correspond to the bottom mixed layer thickness at a given time depending on the history of resuspension, particle settling, and hydrodynamics of bottom waters [Armi, 1978]. Sediment moves along the bottom when the bed shear stress (τ_b; a function of currents, internal waves and surface waves) [*Miller et al.*, 1977; *Grant and Madsen*, 1979; *Cacchione and Drake*, 1986; *Moody et al.*, 1987; *Bogucki et al.*, 1997; *Dickey et al.*, 1998] exceeds a critical value for the sediments in the region (a function of grain size, compaction, cohesion, and organic matter) [e.g., *Miller et al.*, 1977]. For particles to remain in suspension their settling velocity w_s must be less than the shear velocity ($u_* = (\tau_b/\rho)^{0.5}$) generated by currents and waves [*van Rijn*, 1984].

Property-property plots of bulk particle composition reveal information about the source and abundance of particles within the water column. It is impractical, however, to take sufficient water samples to characterize rapidly changes in particle composition in the water column. Fortunately, the composition of particles in water determines the inherent optical properties of water (attenuation, absorption, scattering, and fluorescence). Inherent optical properties are a function of the size, shape, composition, internal structure, index of refraction, and size distribution of particles in the water [*Zaneveld*, 1973], so a change in the correlation between particle and optical properties in time or space signals a change in the type and perhaps the source of particles within a water mass and provides information about mixing or particle dynamics. Thus we can rapidly assess particle properties in the water column by making continuous profiles of inherent optical properties using instruments interfaced with a conductivity-temperature-depth profiler (CTD) [*Pak and Zaneveld*, 1977; *Gardner et al.*, 1985, 1993; *Pak et al.*, 1988; *Siegel et al.*, 1989]. Because of the large dynamic range of optical properties, detailed profiles may help to verify effects of mixing identified from hydrographic data.

Changes in optical properties often occur at the same depth as changes in temperature or salinity, such as at the base of the surface mixed layer or the top of the bottom mixed layer. In fact, the simultaneous change in optical and physical properties substantiates the zone of most recent mixing. However, a correlation between bulk properties of particles and optical parameters may or may not change at the depths of hydrographic/optical changes depending on the source of particles and the mixing history of the water. For example, the depth of the euphotic zone, often defined as the depth of penetration of 1% of the photosynthetically available radiation (PAR) at the sea surface, usually exceeds the depth of the surface mixed layer. Thus biological particles can be produced throughout the euphotic zone and may generate a layer with similar optical and bulk properties whose thickness does not match that of the hydrographic (mixed) layer.

Particles are continuously settling through the water, affecting the composition and distribution (concentration) of particles and their optical response. As a result, the bulk particle composition/optical property correlation in midwater may mimic that in surface waters unless the organic matter is significantly remineralized. Seasonal evolution, deep winter mixing, and storm events can transport or mix surface particles downward or resuspended bottom sediments upward, introducing particles into midwater that are similar in composition to those in surface or bottom waters. The net effect is that layers can be identified on the basis of hydrography, optics, or particle/optical properties, but their boundaries will change on hourly to seasonal timescales as a result of mixing, internal waves, and lateral advection.

Most of the beam attenuation signal in optical profiles in the ocean comes from particles <20 μm [*Pak et al.*, 1988; *Chung et al.*, 1996]. Particles of 20 μm diameter have a settling velocity of <1 m d^{-1} to at most 20 m d^{-1} for dense particles. Thus, while optically sensed particles may not be conservative on long timescales, they can be used as short-term tracers (hours-days) of water masses and mixing when frequent profiles are made [*Gardner et al.*, 1995].

2. Methods

2.1. Instrumentation

Two CMO cruises focused on time series optics and turbulence measurements for 18 days during summer and spring (August 19 to September 9, 1996, aboard R/V *Seward Johnson* and April 20 to May 9, 1997, aboard R/V *Knorr*). Each day, 1-3 consecutive CTD profiles were made morning, noon, and evening at the same location in the center of the CMO study site. A profiling CTD included a SeaTech transmissometer, light backscattering sensor (LSS; spring cruise only), and fluorometer to provide beam attenuation, light backscattering, and chlorophyll fluorescence measurements. In addition, two transects of stations were made across the shelf to the shelf break in the summer, and one transect was made in the spring to extend our spatial coverage. Water samples were analyzed for bulk composition of PM concentration, particulate organic carbon (POC) concentration, and chlorophyll *a* and were correlated with beam attenuation and chlorophyll fluorescence. The optical and particle data were combined with hydrographic data and constitute the focus of this paper. All times reported in this paper are local times (UT minus 4 hours) to maintain the context of the local solar cycle.

Several moorings and bottom tripods were deployed <1 km

from our sampling site to measure atmospheric and surface water conditions, currents, waves, bottom shear stress, and other parameters [*Boyd et al.*, 1997; *Lentz et al.*, 1999; *Dickey and Williams*, this issue; *Chang and Dickey*, this issue]. Regional hydrographic and optical conditions were measured from another ship during our cruises using an undulating profiler [*Barth et al.*, 1998], and satellite imagery was collected during most of the time series measurements [*Porter et al.*, this issue]. An overview of the entire study is provided by *Dickey and Williams* [this issue].

2.2. Physical Measurements

Temperature and salinity data were acquired with a SeaBird 911+ CTD and were binned at 0.5 m intervals. No nighttime hydrocasts were made because the ship was utilized for turbulence measurements during that time. To fill in the nighttime gaps for the summer cruise, data from a microstructure profiler (J. MacKinnon and M. C. Gregg, Summer stratification and solitons: Mixing and internal waves on the New England continental shelf, submitted to *Journal of Geophysical Research*, 2000) were also binned at 0.5 m intervals, and profiles taken every 3 hours were used to match the 3-4 hour intervals of the daytime data. Sections of beam c_p (defined in section 2.3) contain 12 hour gaps at night over which the data are extrapolated. Longer breaks in the data occurred when we left the site for various reasons and are excluded from the plots. MLDs and benthic mixed layers were calculated using a σ_t change of 0.01 kg m^{-3} from the surface and bottom σ_t, respectively.

Bottom current measurements were made from a bottom tripod (Benthic Acoustic Stress Sensors (BASS) data from A. Williams et al., Woods Hole Oceanographic Institution (WHOI), personal communication, 1999). Shear stress and shear velocity due to currents and waves were calculated from the summer BASS data by *Chang et al.* [this issue] based on the model of *Christoffersen and Jonnson* [1985]. The sensors used to calculate wave shear stress were not on the BASS tripod during the spring cruise, but we calculated current shear velocity from the BASS current measurements using the law of the wall equation: $u/u_* = 2.5 \ln (u_* z/\upsilon) + 5.1$, where u is the free stream velocity, u_* is the bed shear velocity, z is the distance above bottom (1.1 m), and υ is the kinematic viscosity of seawater.

2.3. Optical Data

Beam attenuation coefficients were measured using a SeaTech transmissometer (λ = 660 nm), and chlorophyll fluorescence was measured with a SeaTech fluorometer. Attenuation of a light beam was defined by *Jerlov* [1976] as $c = a + b$, where c, a, and b are attenuation, absorption, and scattering coefficients, respectively, all inherent optical properties of seawater with units of m^{-1} [*Zaneveld*, 1973; *Bartz et al.*, 1978]. Beam attenuation across a 25 cm path length (r) transmissometer was obtained by measuring the percent transmission (Tr) of light and using the conversion, $c = -(1/r) \ln (\mathrm{Tr})$. The beam attenuation coefficient is the sum of attenuation due to particles (c_p), water (c_w), and colored dissolved organic matter (c_{CDOM}) [*Pak et al.*, 1988]:

$$c = c_w + c_p + c_{\mathrm{CDOM}} \quad (1)$$

Attenuation due to c_{CDOM} is negligible at 660 nm in open waters [*Bartz et al.*, 1978; *Bricaud et al.*, 1981; *Pak et al.*, 1988], and although it may not be negligible at this shelf site [*Sosik et al.*, this issue], it is a very small contribution (<0.1 m^{-1}) of the total attenuation signal and was neglected in this study.

Assuming that particle properties (size distribution, refractive index, internal structure, shape, and particle composition) remain constant, the attenuation due to particles (beam c_p) is linearly correlated to particle concentration [*Zaneveld*, 1973; *Baker and Lavelle*, 1984; *Gardner et al.*, 1985] using the following equation:

$$c = K_c \mathrm{PM} + c_w, \quad (2)$$

where K_c is the slope of the regression and is a function of particle type, size, and refractive index. The slope may change with depth through the water column as particle types change [*Baker and Lavelle*, 1984; *Gardner et al.*, 1985; *Bishop*, 1986; *Richardson*, 1987; *Gardner*, 1989]. Attenuation due to water is essentially constant and is set at 0.364 m^{-1} for this instrument. However, our minimum value for the cruise was slightly lower (0.350 m^{-1}) on a cast in deep water (~1000 m). This value was assumed to be the "clearest water" and was used as c_w even though it was not particle free.

The LSS measures light backscattering at 880 nm wavelength. Dual light sources and sensors are mounted on the same plane, directed normal to the plane. The light sensors are shielded from the light sources and from low-angle backscattering. Scattering measured with this instrument is not from a specific volume or pathlength, as is the case with a transmissometer. Using an LSS, small particles (37 μm ground glass) scatter four times as much light as large particles (212 μm ground glass) [*Conner and De Visser*, 1992; *Bunt et al.*, 1999], but little information is available about the size sensitivity of smaller natural sediment or in situ particulate matter versus the LSS signal. The backscattering coefficient can be calculated from the particle size distribution and the index of refraction using Mie theory. The ratio of the backscattering to total scattering (assumed here to be nearly proportional to the ratio of the LSS signal to beam c_p) can then be interpreted in terms of these particulate parameters (M. S. Twardowski et al., Retrieving particle composition from the backscatter ratio and spectral attenuation in marine waters, submitted to *Journal of Geophysical Research*, 2000, hereinafter referred to as Twardowski et al., submitted manuscript, 2000).

The relative chlorophyll fluorescence was determined with a SeaTech fluorometer. Chlorophyll a can be related to chlorophyll fluorescence by Chl $a = K_f(\mathrm{Fl}) + b$, where b is an instrumental offset. This regression was used to estimate and contour chlorophyll a as time series sections rather than using fluorescence because the chlorophyll a per unit of fluorescence was much greater in the spring than in the summer, providing a more realistic comparison of spring and summer chlorophyll abundance. Note, however, that there was more chlorophyll b that also contributed to the fluorescence in the spring (C. Roesler, unpublished data, 2000).

2.4. Discrete Water Samples

Water samples were obtained at six depths including the surface mixed layer, chlorophyll maximum, particle minimum, and bottom nepheloid layer. Particulate matter was filtered by in-line vacuum filtration (0.5 atm) by drawing 1-4 L through 47 mm preweighed 0.4 μm Poretics filters. Samples were rinsed with three aliquots of deionized water, dried, reweighed, and corrected using wash blanks.

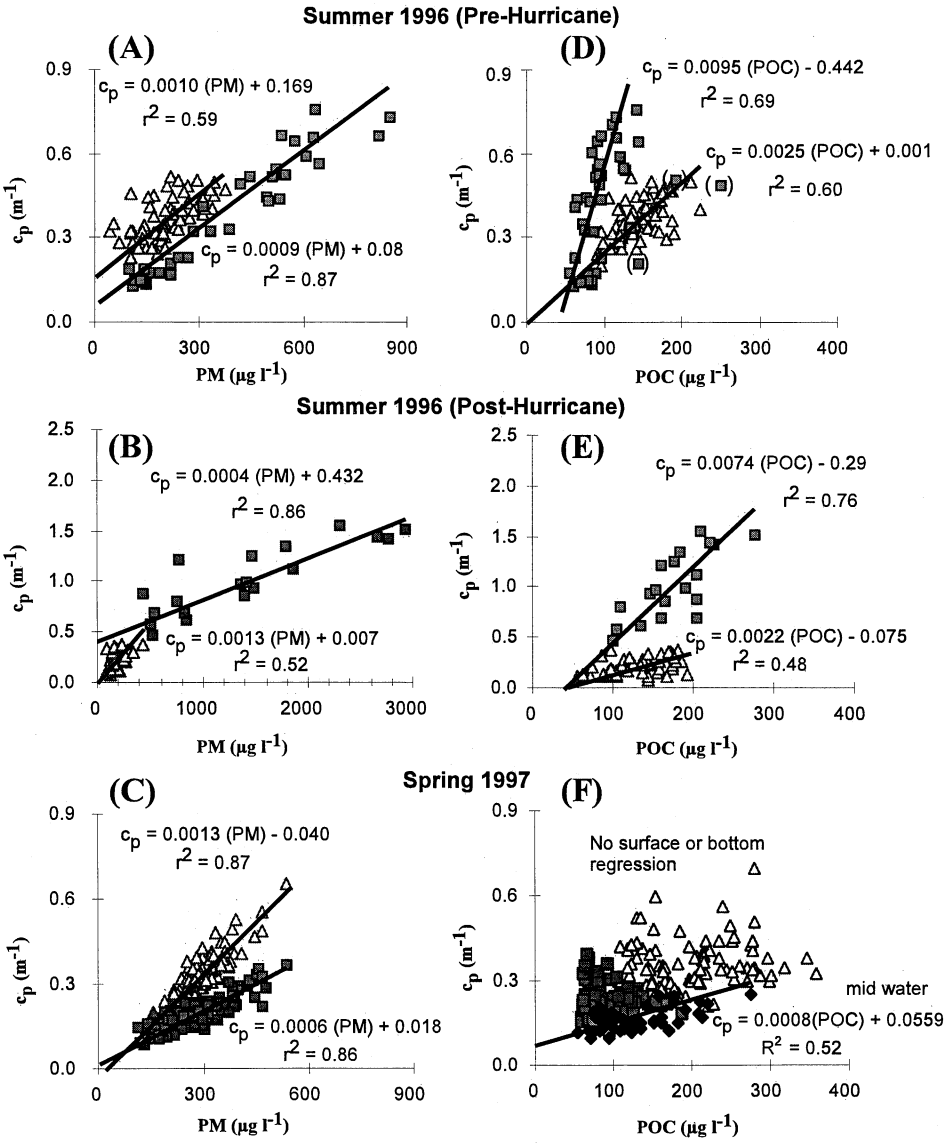

Figure 2. Beam c_p versus PM and POC. Regressions are Model II. Triangles represent surface waters (sea surface to base of chlorophyll maximum) in all panels (~0-30 m in summer and 0-25 m in spring). In Figures 2a and 2d, squares represent samples from bottom waters (>50 m in summer and >35 m in spring), but in other panels squares include midwater samples (~30-50 m in summer and ~ 20-45 m in spring). In Figure 2f the solid diamonds represent samples from midwater (~20-45 m). Linear regressions are shown for r^2 values > 0.35. Linear regression in Figure 2f is for midwater samples. Note the scale change for the posthurricane period.

POC samples were collected in dark 1 L bottles and filtered through precombusted 25 mm glass fiber filters. Samples were dried at 60°C, stored in aluminum foil, and analyzed at the Bermuda Biological Station with an elemental analyzer after acidification to remove inorganic particulate carbon. Chlorophyll *a* samples were analyzed shipboard using standard acetone extraction methods and a Turner fluorometer.

3. Results and Discussion

3.1. Bulk Particle Properties and Optics

3.1.1. Summer. Property-property plots for summer (prehurricane and posthurricane) and spring included beam c_p versus PM and POC concentrations (Figure 2), fluorescence and beam c_p versus chlorophyll (Figure 3), and PM and chlorophyll *a* versus POC (Figure 4). For the spring cruise we also compared LSS with c_p, POC, and PM (Figure 5). Where reasonable (r^2 >0.35), model II linear regressions (regressions where the errors are minimized in both *x* and *y* dimensions, not just in one dimension) were made to quantify the relationships between various optical and bulk particle parameters.

Upon examining the source of different clusters of data on property-property plots it was clear that for many parameters the data could be divided among samples from surface, bottom, and sometimes midwater. These divisions were generally at depths where there were changes in the beam c_p or fluorescence profiles rather than at depths of hydrographic changes (Figures 6 and 7). Midwater values often overlapped between surface and bottom values, so they were sometimes omitted from Figures 2-4 for clarity. For the summer period the water was subdivided into three depth regions: surface (0~30 m),

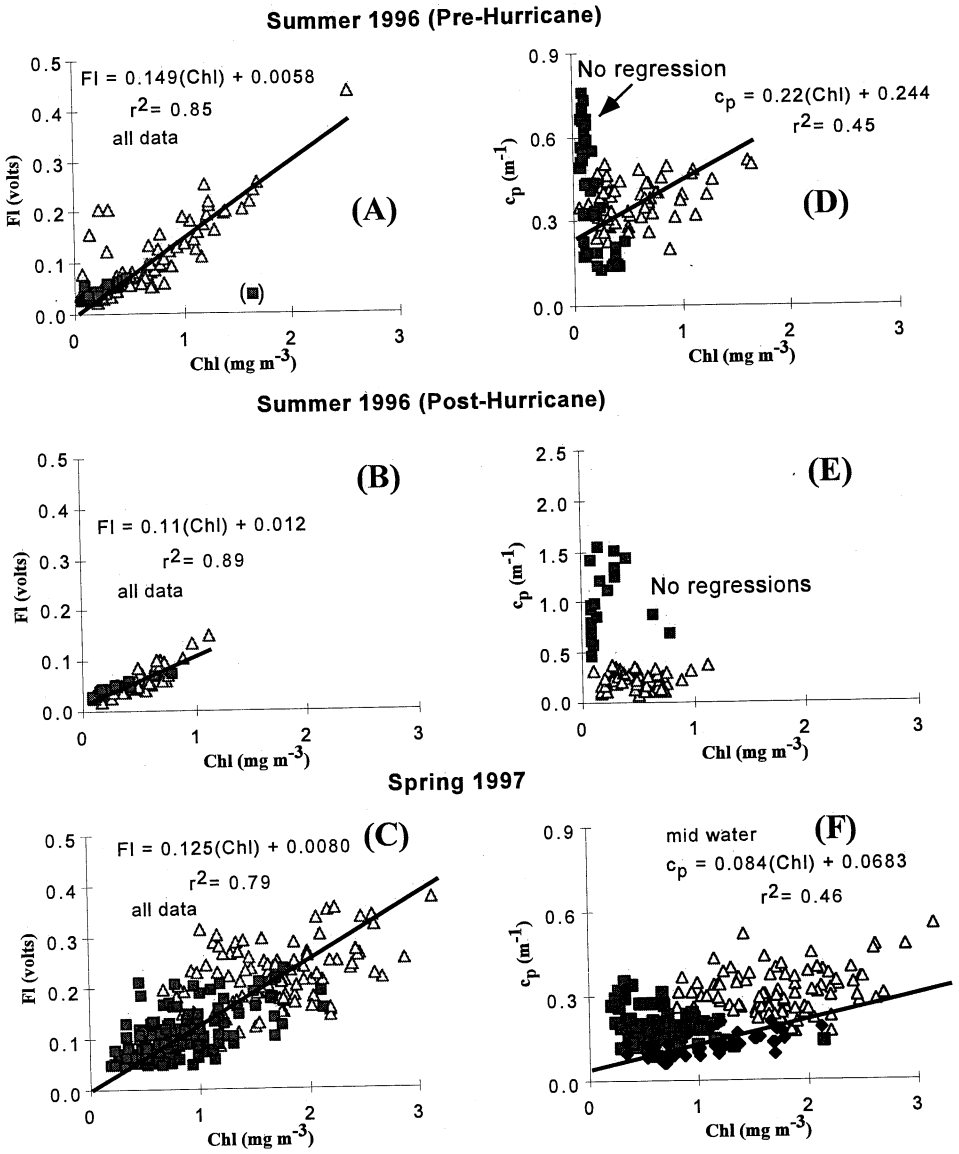

Figure 3. Fluorescence (raw volts) and beam c_p versus chlorophyll. Symbols and regressions are as in Figure 2. In panel Figure 3f the solid diamonds represent samples from midwater (~25-40 m). Note the scale change for the posthurricane period in Figure 3c.

midwater (~30-50 m), and bottom water (50-70 m). These divisions corresponded fairly closely to the base of the subsurface chlorophyll maximum and the depth where beam c_p started to increase near the bottom, i.e., the top of the nepheloid layer. For the spring cruise the water column was similarly subdivided into three regions with some overlap in the depths of the layers because of temporal variations in weakly stratified waters: surface (0~25 m), midwater (~20-45 m), and bottom waters (35-70 m).

The beam c_p/PM, c_p/POC, and PM/POC correlations prior to the hurricane (Figures 2a, 2d, and 4a and Table 1) showed distinct differences between particles in surface and bottom waters, with more scatter in surface than bottom waters. The differences are strong evidence for two different particle sources. The regression of raw fluorescence to chlorophyll was strongly correlated, with no distinctions between surface, midwater, and bottom waters (Figures 3a-3c). The Chl/fl ratio represents the efficiency of chlorophyll fluorescence and depends on the phytoplankton physiology and speciation, including organism size and internal structure and the presence of detrital and accessory pigments [*Zaneveld et al.*, 1982; *Marra*, 1997; *Sosik et al.*, this issue].

The various ratios presented here can be interpreted in terms of bulk particulate properties. The ratio of the particulate attenuation to the total particulate mass (c_p/PM) is a parameter that increases with the slope of the particulate size distribution (i.e., a higher value of a Junge-type hyperbolic slope of particle size distribution, which means more small particles) and with the average index of refraction [*Baker and Lavelle*, 1984; *Spinrad*, 1986]. Ratios of c_p/PM were similar in surface and nepheloid layer waters prehurricane but were about 3 times greater in surface waters posthurricane (Figures 2a and 2b). The hurricane resuspended bottom sediments, and the thickness of the nepheloid layer increased, increasing PM concentration in

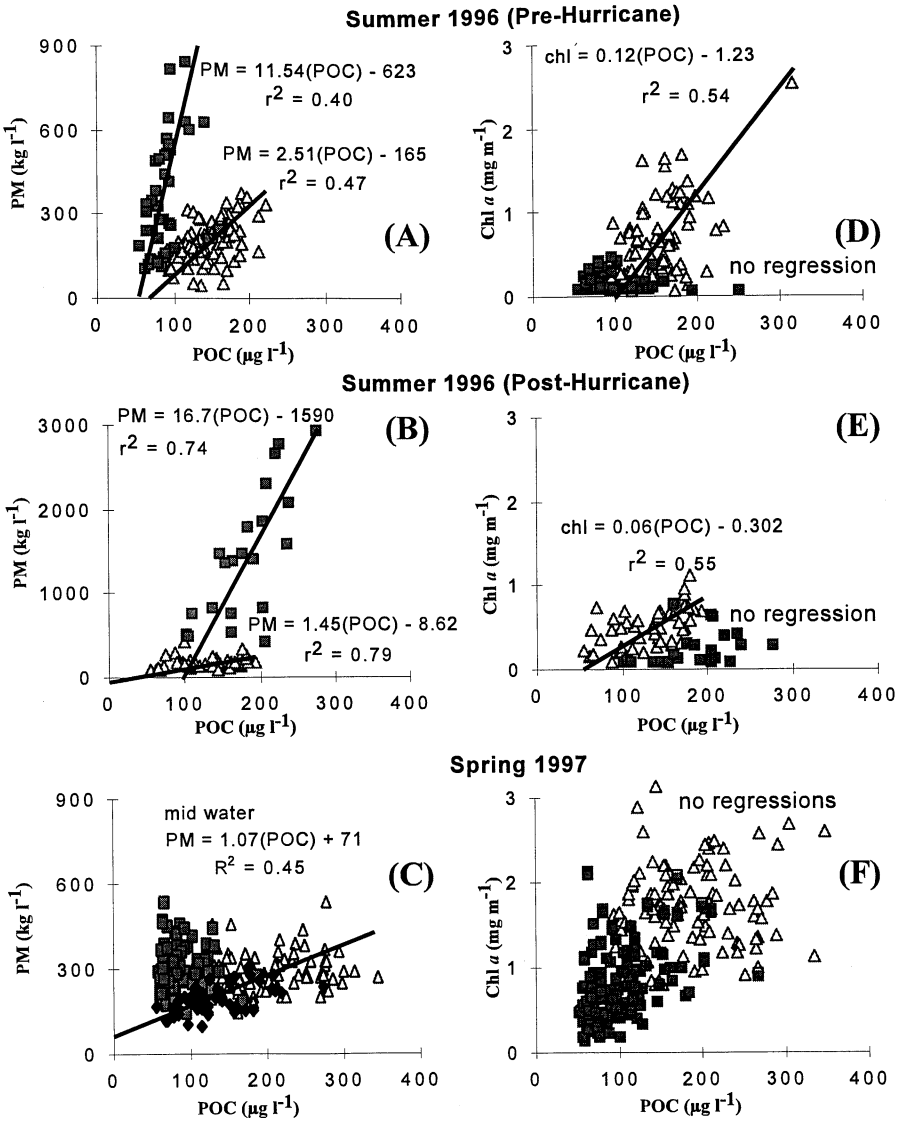

Figure 4. PM and chlorophyll versus POC. Symbols and regressions are as in Figure 2. The squares represent midwaters and bottom waters except in Figure 4d where midwater values were highly scattered (not shown) and in Figure 4c where the solid diamonds represent samples from midwater (~25-40 m). Note the scale change for the posthurricane period in Figure 4b.

bottom waters from 800 to 3000 μg L^{-1}. More significant was the posthurricane decrease in the c_p/PM regression slope from 9 x 10^{-4} to 4 x 10^{-4}, suggesting a shift to larger particles a few days after the hurricane passed. *Hill et al.* [this issue] found that the number of large aggregates 1 m above bottom decreased during the hurricane but quickly increased after its passage. With a tripling of particle mass in the water column the size and abundance of aggregates could increase quickly when extremely high shear rates decreased after the hurricane passed.

The PM/POC ratio is inversely proportional to the percentage of organic material in the total particulate matter. Because organic matter has a lower index of refraction than mineral matter, we infer that the ratio of PM/POC is inversely proportional to the average index of refraction of the particles. With PM/POC ratios 5-12 times greater in bottom waters than in surface waters, particles in surface waters clearly have a lower index of refraction than the nepheloid layer particles (Figures 4a and 4b). As noted above, the c_p/PM ratios were similar in surface and bottom waters prehurricane. Since the PM/POC ratio suggested particles in surface waters had a much lower bulk index of refraction than those in the nepheloid layer, we conclude that prehurricane surface water particles must have been smaller relative to particles in bottom waters to account for the similar c_p/PM values (Figure 2a). Posthurricane c_p/PM values were ~3 times greater in surface waters than in nepheloid layer waters, suggesting that posthurricane particles in surface waters were also smaller than those in the nepheloid layer.

3.1.2. Spring. In spring, beam c_p and PM were well correlated, especially in surface waters (Figure 2). Midwater values overlap the low concentration end of the bottom water values. Slopes of the regressions are distinctly different in surface and deep waters, unlike the summer period. This

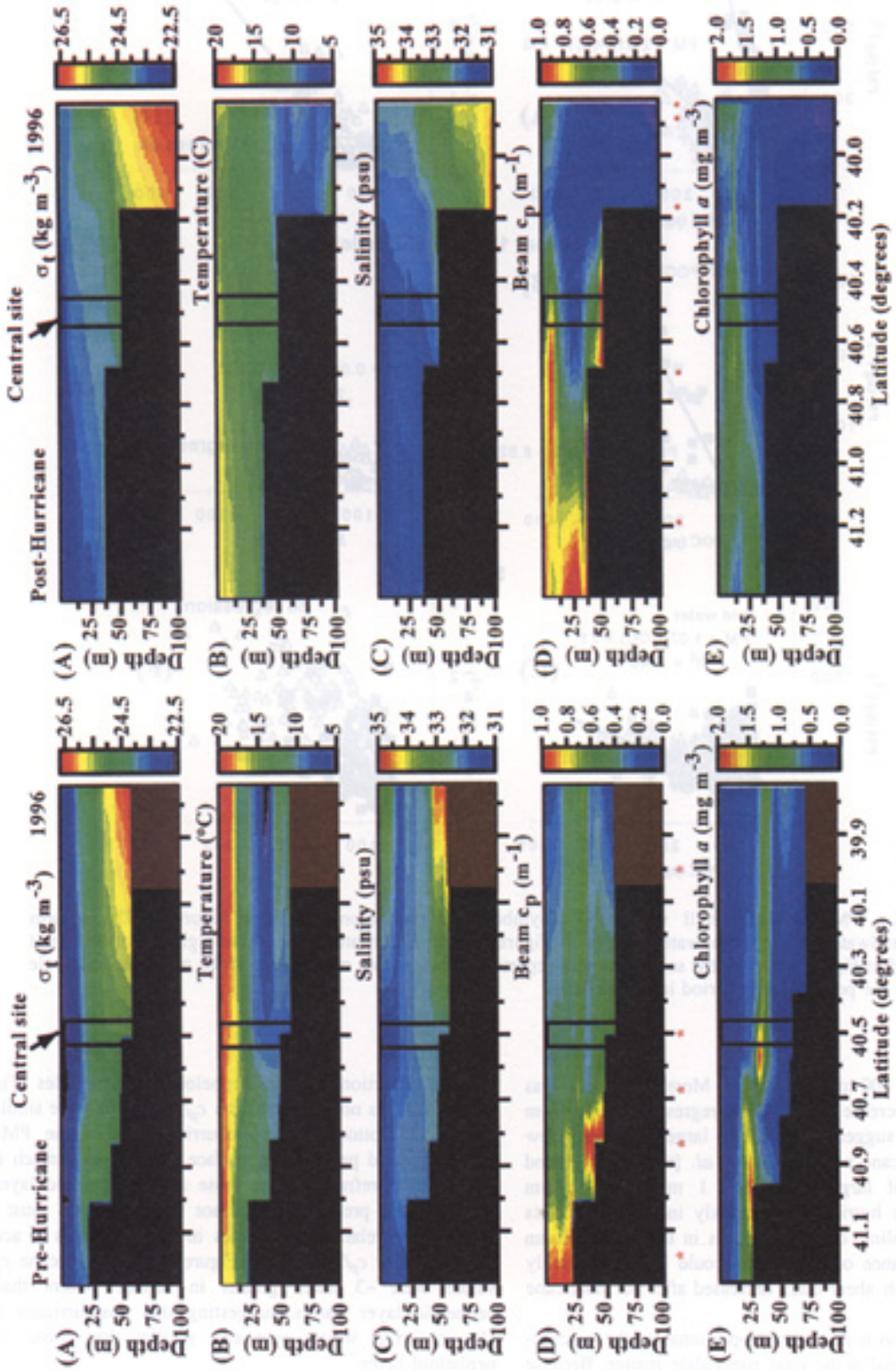

Plate 1. Cross-shelf sections for prehurricane period (August 17-18, 1996). The asterisks below Plate 1d indicate station locations. The double bars represent our time series site. Brown covers areas with insufficient data to contour.

Plate 2. Cross-shelf sections for posthurricane period (September 5-7, 1996). The asterisks below Plate 2d indicate station locations.

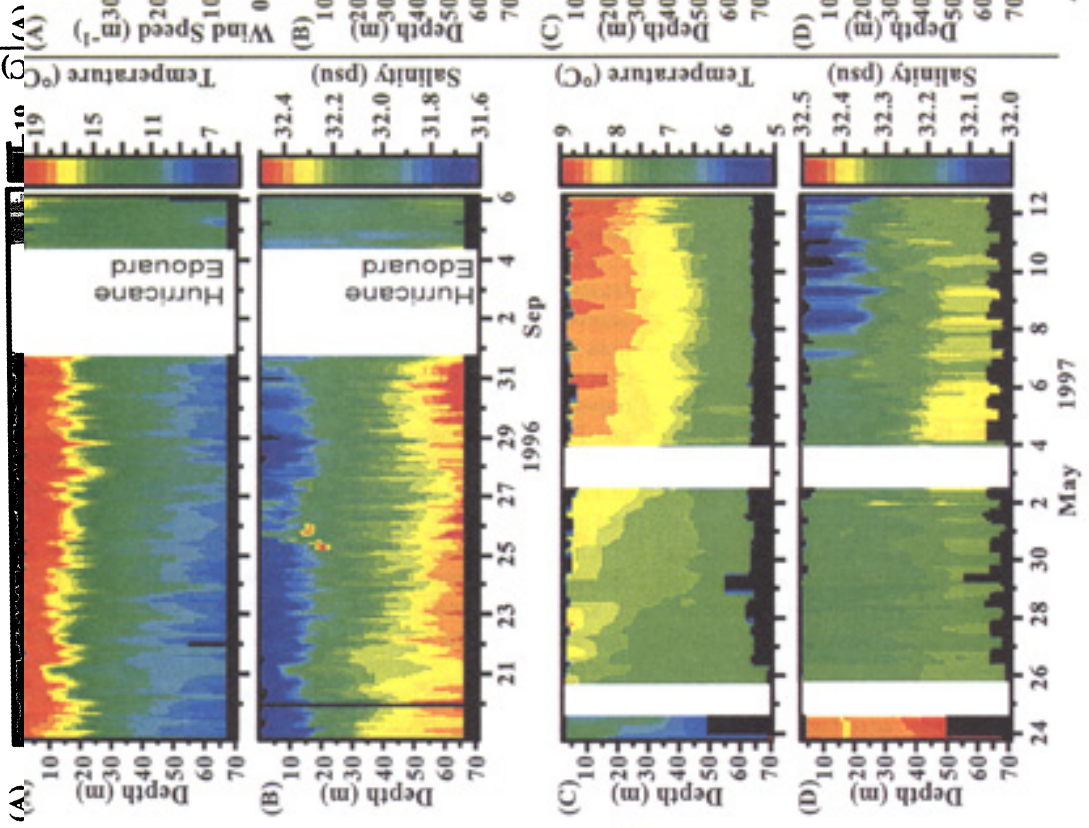

Plate 3. Time-series sections of (a) wind speed and wave height (data from S. Anderson et al., WHOI, personal communication, 2000), (b) σ_t, (c) beam c_p, and (d) chlorophyll for the summer 1996 cruise. The 0.01 $\Delta\sigma_t$ MLD (red line) and 0.01 $\Delta\sigma_t$ BML (black line) are plotted on Plates 3b and 3c. The depth of the 10% PAR light intensity (yellow line) and 1% PAR light intensity (red line) are plotted on Plate 3d.

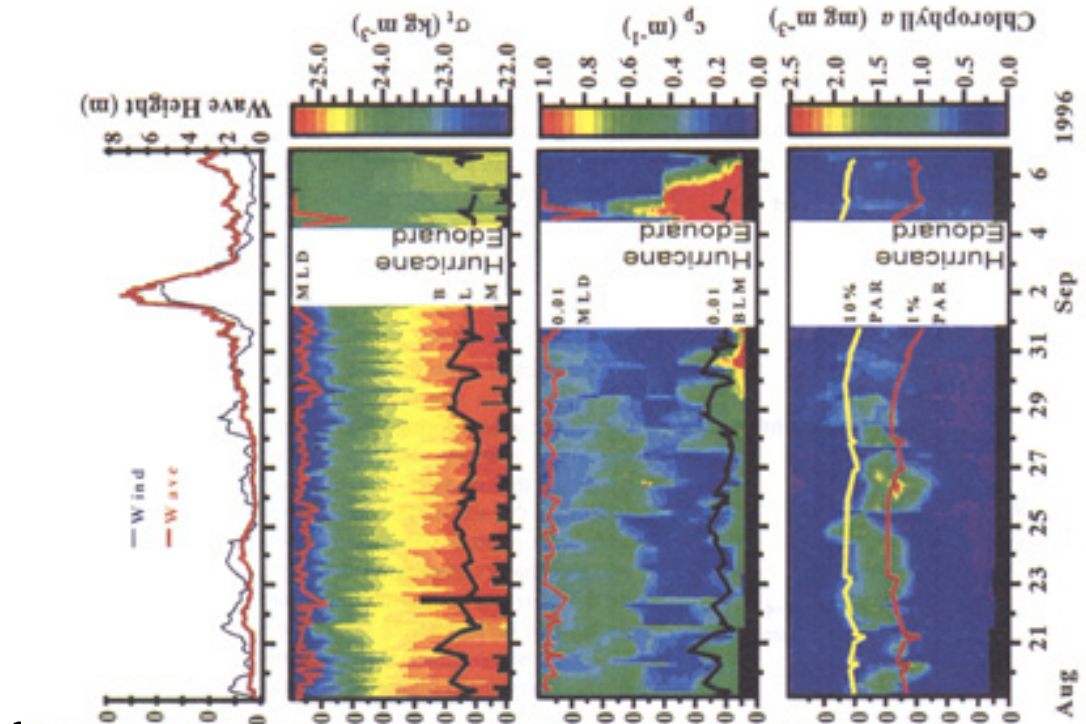

Plate 4. Time series sections of (a) temperature and (b) salinity for the summer 1996 cruise and (c) temperature and (d) salinity for the spring 1997 cruise. Note the different scales for the spring cruise (Plates 4c and 4d).

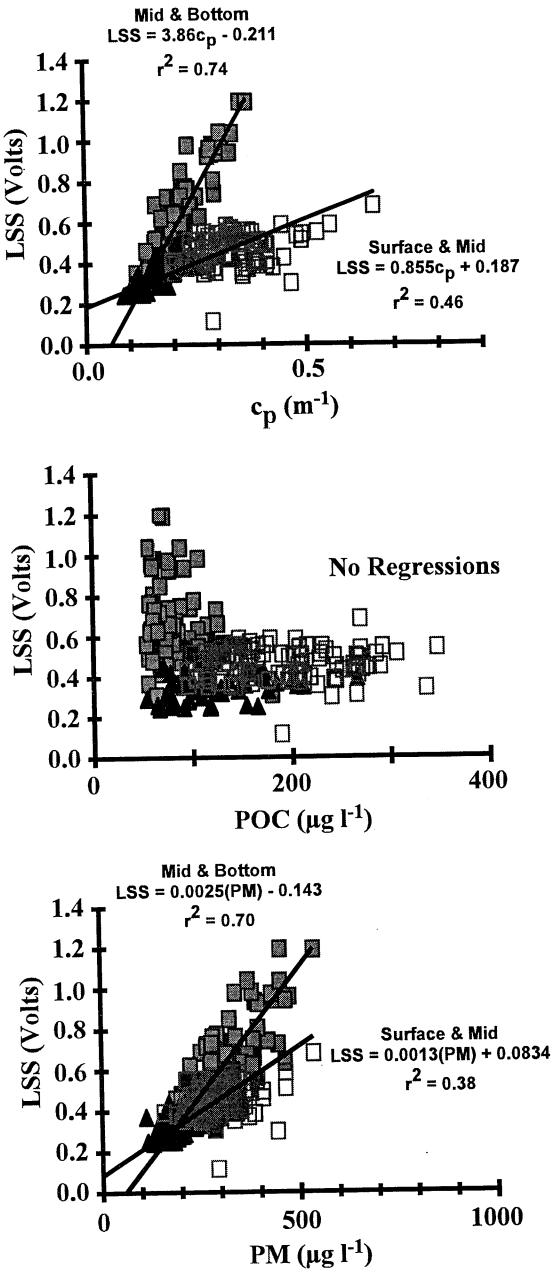

Figure 5. LSS versus beam c_p, POC, and PM for the spring cruise. Symbols and regressions are as in Figure 2.

suggests distinctly different particle types and greater mixing and uniformity of particle composition within each layer of the weakly stratified water column. Correlations were poor for c_p/POC, c_p/chlorophyll, PM/POC, and chlorophyll/POC, even though the data were subdivided at the base of the high-chlorophyll zone (Figures 2-4). The primary trend was that chlorophyll and POC concentrations were higher in surface waters because of higher biological productivity near the surface. Fluorescence and chlorophyll seemed to be similarly correlated at all depths, so all data were included in a single regression for each cruise (Figures 3a-3c). The increased scatter during the spring may be due to changing amounts of fluorescence per unit chlorophyll as the bloom progressed [*Sosik et al.*, 1998].

The backscatter b_b to attenuation c_p ratio was much smaller in surface waters than in bottom waters (Figure 5a). *Hall et al.* [2000] observed this same relationship and attributed the difference to the presence of more large particles in surface waters than in deep waters. However, our direct measurements of particle size distribution show that in the 1-20 μm size range, particles were often smaller in surface than in deeper waters [*Blakey*, 1999]. Furthermore, analysis of Twardowski et al. (submitted manuscript, 2000) suggests that the bulk index of refraction may be the primary reason for the difference rather than particle size. They demonstrated that the ratio b_b/b_p of backscattering b_b to particulate forward scattering b_p increases with the average index of refraction and with the slope of the size distribution. LSS/c_p is proportional to b_b/c_p, and c_p at 660 nm is almost entirely due to scattering b_p, though this decreases slightly in high-chlorophyll waters. Thus LSS/c_p is nearly proportional to b_b/b_p. The parameter b_b/b_p increases with the average index of refraction and with the slope of the size distribution. We can thus conclude that the surface waters during CMO contained larger or lower refractive index particles than the deeper particles. We already concluded that changes in c_p/PM were due to particles being smaller at the surface in both spring and summer, consistent with direct particle size measurements. Thus the surface particles must have a smaller index of refraction, which is expected for a higher concentration of organic particles, causing the decrease in backscattering in surface waters.

A secondary effect may be more light absorption a in surface waters from higher concentrations of chlorophyll-rich biogenic particles. Attenuation is the sum of absorption and scattering, and while scattering is by far the larger component, the absorption contribution increases in surface waters [*Sosik et al.*, this issue]. The LSS measures only scattering, not absorption, so differences will be largest between LSS and beam c_p in regions where absorbing particles are present, i.e., chlorophyll-rich waters. Thus one would expect a smaller LSS/c_p ratio in surface waters where chlorophyll is abundant, particles are smaller, and the index of refraction is smaller.

3.1.3. Summer/spring comparisons and contrasts. Several differences were observed between the summer and spring data. Surface water PM and POC concentrations were greater in spring than in summer. Bottom water PM concentrations were greater in the summer, and POC concentrations were similar (Figure 2). The correlations between c_p and PM were strong in both the surface and bottom waters (Figures 2a-2c). There was considerably more scatter in plots of PM versus POC in spring than in summer (Figures 4a-4c) and in c_p versus POC (Figures 2d-2f).

Chlorophyll concentrations were 2-3 times greater in spring than in summer throughout the water column (Figure 3). A strong relationship was seen between chlorophyll and fluorescence during both time periods, though there was more scatter in the data in spring than in summer. We speculate that the increased scatter may indicate greater variance in community structure and photoadaptation during an active bloom than occurs in late summer. The bulk chlorophyll/fluorescence relationship showed little change with depth.

In correlating POC and PM data with beam c_p it was apparent that at least two particle populations were necessary to explain the data distribution: particles from above and below the chlorophyll layer in both seasons (Figure 2). The change in correlations between layers results from a change in particle

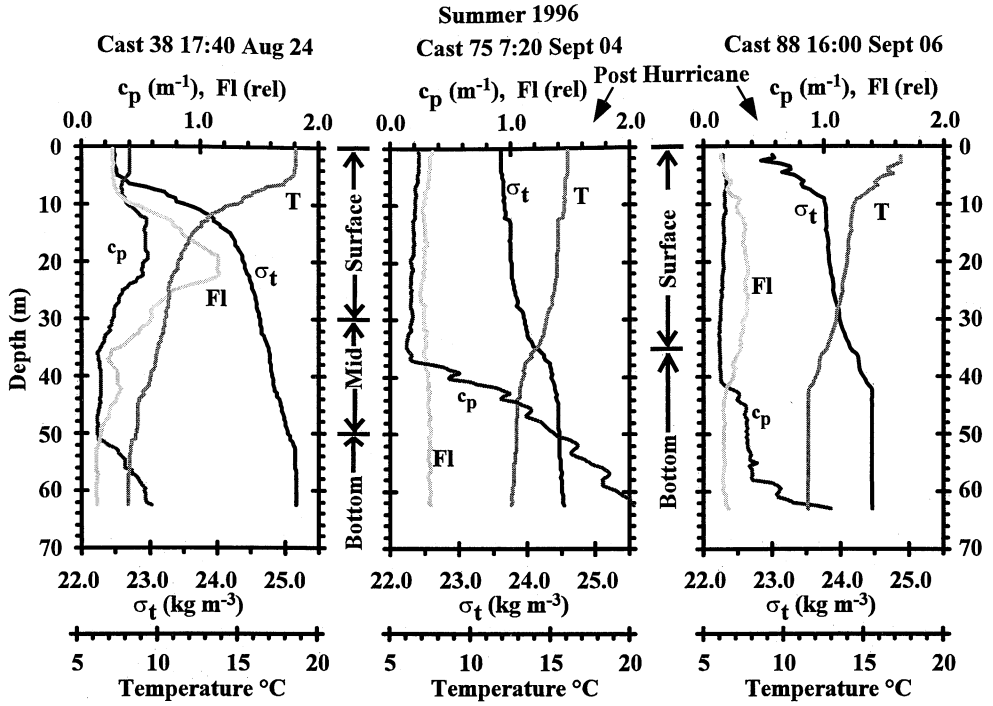

Figure 6. Profiles of σ_t, temperature, beam c_p, and fluorescence prior to the hurricane, immediately after the hurricane passed, and 2 days later. Classification of surface, midwater, and bottom waters was based on bulk particle properties and optical parameters, not on σ_t.

type, size, or composition (see explanation above). Phytoplankton were abundant in surface waters during both summer and spring [*Sosik et al.*, this issue] and were the primary source of particles. The percentage of organic matter decreased with depth as POC was remineralized as plankton died or were ingested. These particles depleted in POC settle to underlying waters and were a source of particles in that region. During both spring and summer the percentage of POC decreased from 50-90% in surface waters to 10-50% in bottom waters. Resuspended sediments provide a second source of particles to

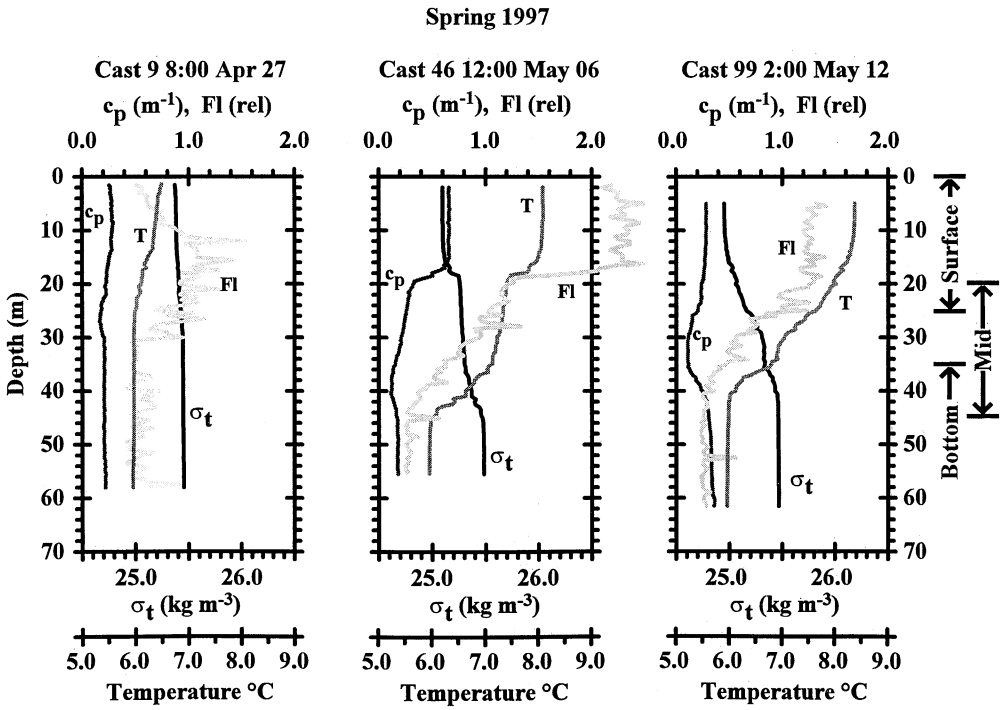

Figure 7. Profiles of σ_t, temperature, beam c_p, and fluorescence at the beginning, middle, and end of the spring cruise. Classification of surface, midwater, and bottom waters was based on bulk particle properties and optical parameters, not on σ_t.

Table 1. Slope m, Intercept b, and Correlation of Optics and Bulk Particle Properties

Depth Zone	c_p/PM			c_p/POC			PM/POC			LSS/PM			LSS/c_p			Fl/Chl			c_p/Chl			Chl/POC		
	m	b	r^2	m	b	r^2	m	b	r^2	m	b	r^2	m	b	r^2	m	b	r^2	m	b	r^2	m	b	r^2
Summer pre-H																								
surface																			0.2200	0.2400	0.45	0.120	-1.230	0.54
surface and middle	0.0010	0.1690	0.59	0.0025	0.0010	0.60	2.51	-165.0	0.47															
bottom	0.0009	0.0800	0.87	0.0095	-0.4420	0.69	11.54	-623.0	0.40							0.1460	0.0058	0.85						
all depths																								
Summer post-H																								
surface	0.0013	0.0070	0.52	0.0022	-0.0750	0.48	1.45	-8.6	0.79													0.060	-0.302	0.55
surface and middle																								
middle and bottom	0.0004	0.4320	0.86	0.0074	-0.2900	0.76	16.70	-1590.0	0.74							0.1100	0.1200	0.89						
all depths																								
Spring																								
surface	0.0013	-0.0400	0.87							0.0013	0.08	0.38	0.0855	0.187	0.46									
middle				0.0008	0.0560	0.52	1.07	71.1	0.45										0.0840	0.0680	0.46			
middle and bottom	0.0006	0.0180	0.86							0.0025	-0.14	0.7	3.86	-0.21	0.74	0.1250	0.0080	0.79						
all depths																								

bottom waters that are compositionally distinct from settling phytodetritus, resulting in the much larger c_p/POC slopes for deep samples (Figures 2d and 2e) since surface sediments have a substantially lower POC/PM ratio. The decrease in percent organic matter produces a different optical response [*Zaneveld et al.*, 1982; *Kitchen and Zaneveld*, 1990; *Morel*, 1991; *Iturriaga et al.*, 1991; *Chung et al.*, 1998; *Claustre et al.*, 1998].

3.2. Hydrography and Optics

3.2.1. Cross-shelf transects: Summer 1996. The general hydrographic and atmospheric conditions during our study were similar to those reported from previous years and discussed earlier. As seen in the first cross-shelf transect that was completed at the start of the summer period, summer waters were strongly stratified and the cold pool was well developed seaward of the 50 m isobath (Plate 1; compare with Plate 2 after the passage of a hurricane). The CMO sampling site was at the northern end of the cold pool. The entire water column was strongly stratified and contained a well-defined subsurface chlorophyll maximum that merged with the bottom layer at the northern end of the transect. Stratification decreased in shallower water but was always present.

3.2.2. Hydrography and atmospheric conditions: Summer time series. Sections of temperature and salinity (Plate 3) showed well-stratified waters for the first 2 weeks of the study. Relatively calm, sunny weather, with only one major rain event, prevailed prior to the hurricane (A. Plueddemann et al., unpublished data, 2000). Mean seasonal currents were westward at 5-10 cm s^{-1} and offshore at about 6 cm s^{-1} at the surface, decreasing to 1 cm s^{-1} at 10 m and deeper [*Lentz et al.*, 1999]. Winds were generally <5 m s^{-1}, and mean wave heights were <2 m (Plate 4). An unexpected scientific bonus for a study of mixing was the occurrence of Hurricane Edouard (September 1, 1996), which passed within 110 km of the central site [*Dickey et al.*, 1998], obliterated the cold pool, and rapidly mixed and stirred the water as observed in a transect completed about 4 days after the passage of Hurricane Edouard (Plate 2). The wind increased to a sustained speed of 25 m s^{-1} during the height of the hurricane, decreasing to ~ 5 m s^{-1} after the passage. Long-period swell heights increased to nearly 3 m during the 3-4 days before the hurricane and 5-6 m during the hurricane. In the 4 days following the hurricane, swells remained high from the passage of Hurricane Edouard (110 km from eye) and the approach of Hurricane Hortense (September 14, 1996), which passed within 350 km of the CMO site.

The water column was strongly stratified, with a top to bottom $\Delta\sigma_t$ of 3.0 kg m^{-3} prior to Hurricane Edouard (Plate 4). The main pycnocline started at a depth of 5-10 m and was 10-20 m thick prior to the hurricane. After the hurricane the water column was mixed to a quasi two-layer system with $\Delta\sigma_t$ of only 0.8 kg m^{-3} and slight stratification within each layer (Figure 6). Surface temperatures dropped from 21° to 15°C, and bottom waters increased from 7° to 11°C (Plate 3). The surface water began to warm and restratify as soon as the hurricane passed, but advection also readjusted water masses.

Depths of specific PAR light intensities remained fairly constant throughout the summer cruise (Plate 4). The depth of 10% PAR light intensity was between 17 and 22 m, and the depth of 1.0% PAR light intensity was between 32 and 41 m. No significant change was observed after the hurricane.

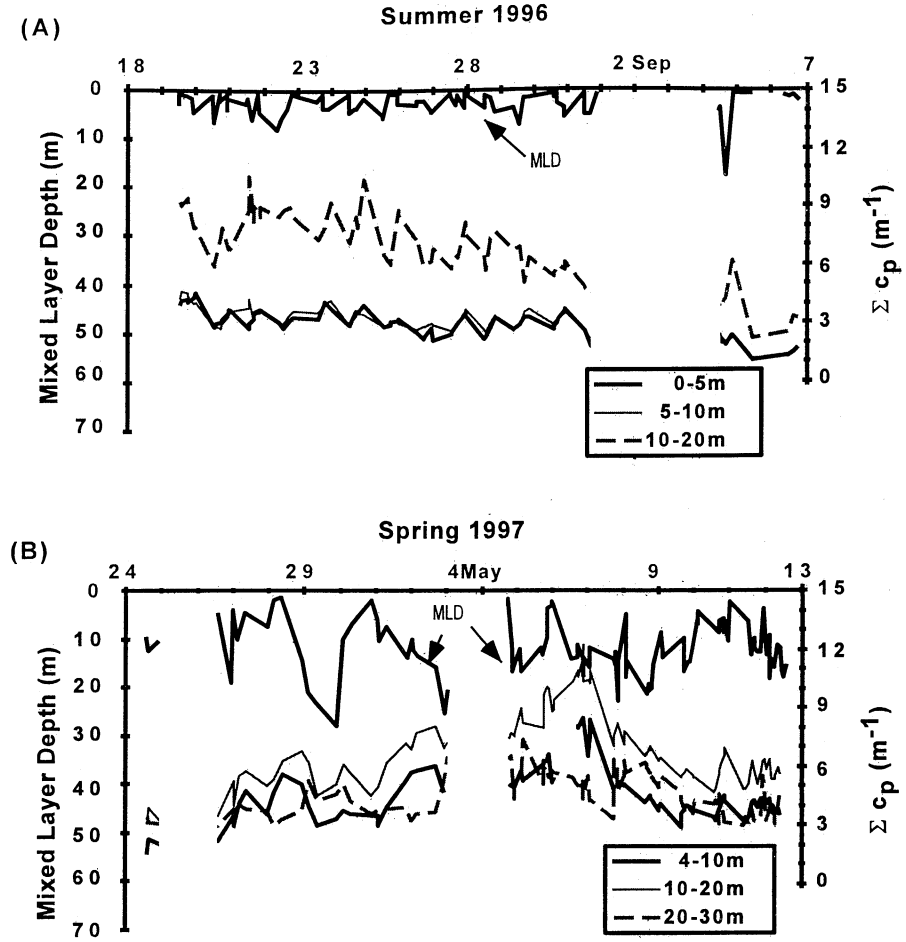

Figure 8. MLD and integration of beam c_p over discrete surface intervals for (a) summer and (b) spring cruises. Diel fluctuations in integrated c_p are observed throughout the water column during the summer and may be related to tidal oscillations rather than to changes in MLD.

3.2.3. Beam c_p and chlorophyll distributions: Summer 1996. During the highly stratified summer period, chlorophyll ranged from 0.5 to 2.5 mg m^{-3} in upper waters with a subsurface chlorophyll maximum between 20 and 40 m with chlorophyll isopleths generally following σ_t isopleths (Plate 4). The depths of the 10 and 1% PAR light intensities (Plate 4) bound the chlorophyll maximum. A subsurface maximum in beam c_p was associated with the chlorophyll maximum, but the c_p maximum occurred some 5 m above the chlorophyll maximum, on average (see Figure 6). This is as expected [*Kitchen and Zaneveld*, 1990] because of photoadaptation of phytoplankton. This correlation, plus bulk measurements of particle composition (high POC/PM values and high Chl/POC values; Figure 4) and discrete particle analysis [*Sosik et al.*, this issue], indicate that most of the particles in the upper waters were of biogenic origin. A subsurface chlorophyll maximum is a common feature of surface waters under stratified conditions [*Hobson and Lorenzen*, 1972; *Marra*, 1997]. Chlorophyll decreased throughout the water column 2 days before Hurricane Edouard. Chlorophyll concentrations were still below prehurricane levels at the end of our cruise (Plate 4), but a small subsurface peak in chlorophyll began to develop as surface water stratified in the two sampling days after the hurricane.

3.2.4. Mixed layer depths. MLDs are generally correlated with wind stress [*Weller*, 1981] but are influenced by the degree of stratification and nighttime convective cooling. MLD (based on a 0.01 kg m^{-3} decrease in σ_t) was typically <10 m and in many instances <5 m with fluctuations of only 2 or 3 m between day and night depths with little variation apparent from atmospheric forcing before the hurricane (Plate 4). Occasionally, the MLDs actually appeared to deepen during the day and decrease at night, contrary to what would be expected for normal daytime heating and nighttime convective cooling and mixing [*Brainerd and Gregg*, 1995]. During the summer cruise the heat flux calculated from moorings data by A. Plueddemann et al. (unpublished data, 2000) indicated that the net heat flux was always into the ocean during the day, but the net heat flux was often out of the ocean during the night because the long-wave radiation was large. Apparently, the net result was that the strong density gradients and low, quasi steady energy input from both wind and waves, prevented the MLD from varying significantly. Furthermore, advection of surface water with lower density can stratify the water [*Tandon and Garrett*, 1996]. The hurricane caused significant mixing, but 2 days after the hurricane the MLD was similar to prehurricane conditions (Plate 4).

Changes in MLD can accelerate downward mixing of parti-

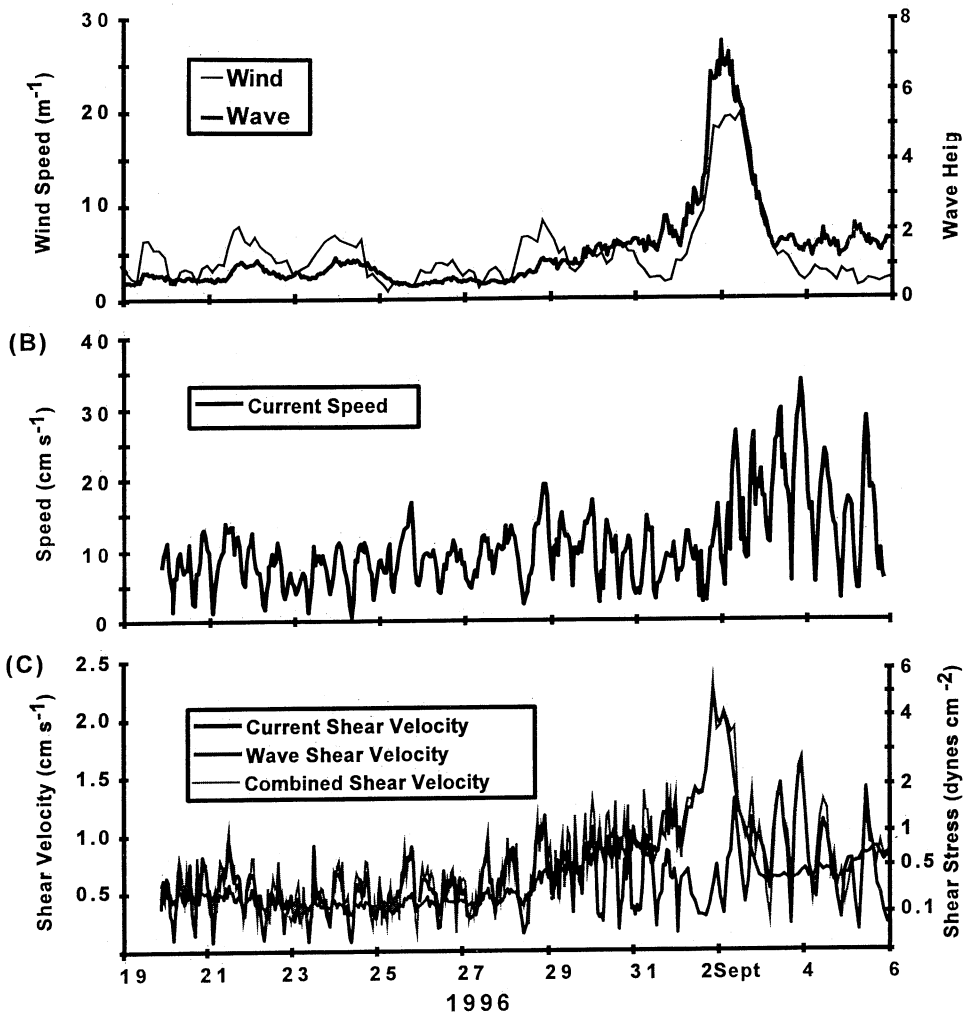

Figure 9. (a) Wind and wave height (data from S. Anderson et al., WHOI, personal communication, 2000), (b) current speed at 1.1 m above bottom (data from A. Williams et al., personal communication, 2000), and (c) shear velocities calculated by *Chang et al.* [this issue] for the summer 1996 cruise. Shear velocities are broken into components because of waves and currents and the combined wave and current shear.

cles and entrainment of deeper, low particle concentration waters from depth [*Gardner et al.*, 1995]. During our summer CMO measurements, day to day changes in beam c_p in the mixed layer were usually <0.05 m^{-1}. To test further for temporal changes in small-particle load, we integrated beam c_p over selected depths (Figure 8). Integration of beam c_p from 0 to 5 or 5 to 10 m showed little change. Because the MLD varied so little during the summer, it is unlikely that MLD changes had much impact on particle settling. There was a decrease in the integrated beam c_p from 10 to 20 m, especially after the hurricane passed. Temporal oscillations in integrated beam c_p were larger between 10 and 20 m than at shallower depths and appeared to follow a daily cycle [*Blakey*, 1999], suggesting periodic (tidal?) oscillation of a water mass (see current data of *Chang and Dickey* [this issue]) in which there were lateral particle concentration gradients.

3.2.5. Bottom nepheloid layer dynamics. The bottom mixed layer (BML) was between 10 and 15 m thick (based on the same criterion of a decrease in σ_t of 0.01 kg m^{-3} from the bottom water). A distinct bottom nepheloid layer (where c_p increases with depth) was present near the seafloor throughout the sampling period (Figure 6 and Plate 4c). The BML height generally encompassed the nepheloid layer thickness, but it was not a strictly constraining boundary. At times the nepheloid layer thickness exceeded the BML, primarily during the 4 days before Edouard arrived when large, long-period surface swells were present. The largest beam c_p values were in the bottom nepheloid layer and ranged from 0.3 to 0.8 m^{-1} in the first 10 days, increasing to 1.5 m^{-1} in the 3 days before Hurricane Edouard arrived. Two days after the hurricane the BML thickness was similar to prehurricane conditions (Plate 4).

Nepheloid layers are caused by resuspension of sediments either locally or advected after resuspension elsewhere. In order to resuspend sediment the critical shear velocity for transport and suspension of surface particles must be exceeded. For a 10 μm grain the critical shear velocity is 0.6 cm s^{-1}; for 63 μm the shear velocity must exceed 1.0 cm s^{-1} [*Miller et al.*, 1977]. To remain in suspension, shear velocity must exceed particle settling velocity ($u* > w_s$) [*van Rijn*, 1984]. Stokes

settling velocities for mineral grains of 10 and 63 μm are ~0.005 and ~0.1 cm s^{-1}, respectively. Grain size analysis revealed that nearly all sediment grains in this area were <63 μm, and 50% were <32 μm, and most particles in the nepheloid layer were <10-20 μm [*Blakey*, 1999]. Near-bottom currents were between 2.5 and 25 cm s^{-1} prior to the hurricane, yielding a current shear velocity between 0.1 and 1.0 cm s^{-1}. The wave shear velocity was of the order of 0.5 cm s^{-1} before Hurricane Edouard (Figure 9) [*Dickey et al.*, 1998; *Chang et al.*, this issue; *Hill et al.*, this issue]. Thus the combined current and wave shear velocity regularly exceeded the 0.6 cm s^{-1} threshold for transport throughout the summer sampling period and $u* > w_s$, so beam c_p increases in the nepheloid layer could be attributed to local resuspension (Figure 9).

3.2.6. Effects of Hurricane Edouard. The effects of the hurricane on the shelf became evident long before the high winds of the hurricane arrived (Plate 4). During the 3-4 days prior to the closest approach of Hurricane Edouard, long-period wave activity increased, bottom isopycnals shoaled, and nepheloid layer thickness and particle concentration increased. Prior to the hurricane, bed shear stress was induced mostly by bottom currents (Figure 9c). In the several days before the hurricane, current shear velocity increased slightly; however, the wave shear stress increased even more than current shear stress both relatively and in absolute magnitude (Figure 9c). *Dickey et al.* [1998] found a better correlation in their moored instrument data between near-bottom beam c_p and current shear stress than between c_p and wave shear stress and concluded that resuspension of bottom sediments was dominated by currents rather than waves. They also estimated a critical bed shear stress of 0.8 dyn cm^{-2} (shear velocity = 0.88 cm s^{-1}) from their data. We plotted beam c_p at the bottom of each CTD profile versus the current and wave shear stress closest to the profile time (Figure 10) and suggest that while beam c_p does not remain high until shear stress exceeds 0.8 dyn cm^{-2}, beam c_p remains high after wave shear stress exceeds 0.3 dyn cm^{-2}. This is consistent with the increase in nepheloid layer beam c_p when long-period surface waves dramatically

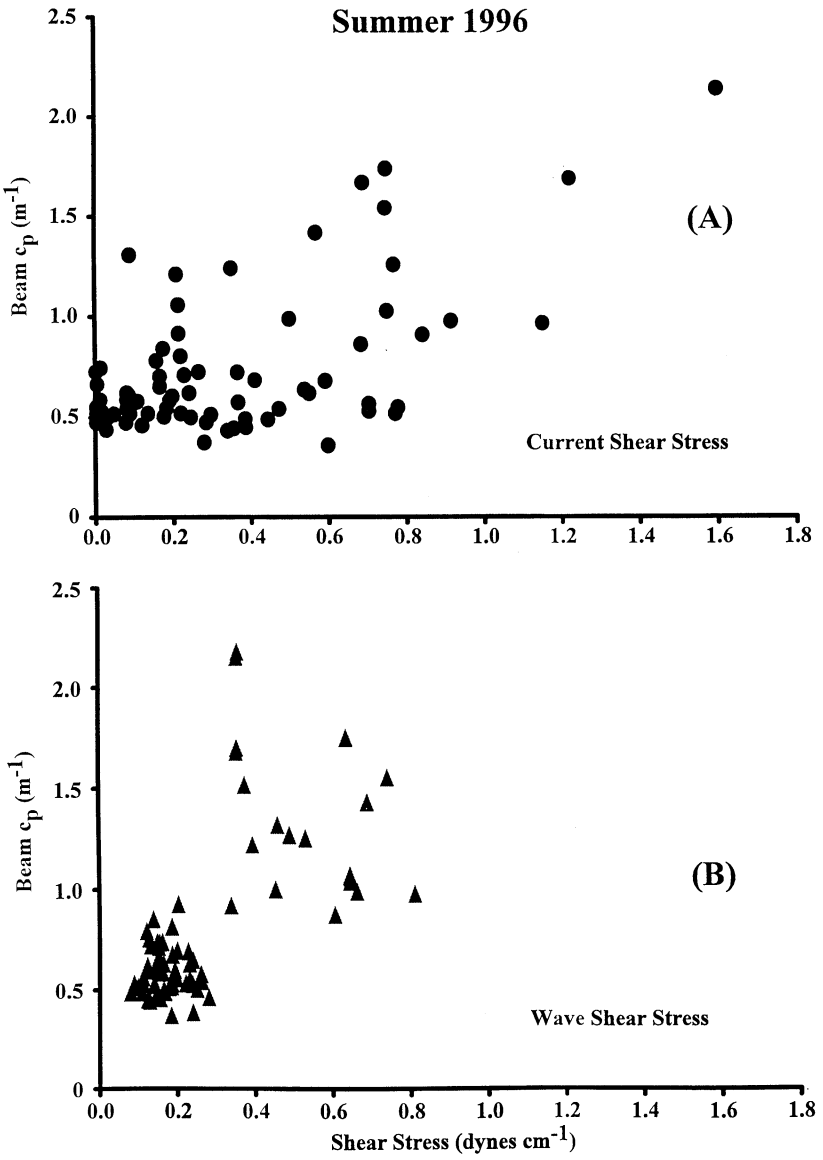

Figure 10. Beam c_p at the bottom of each CTD profile as a function of (a) current shear stress and (b) wave shear stress. Shear stresses are from *Chang et al.* [this issue].

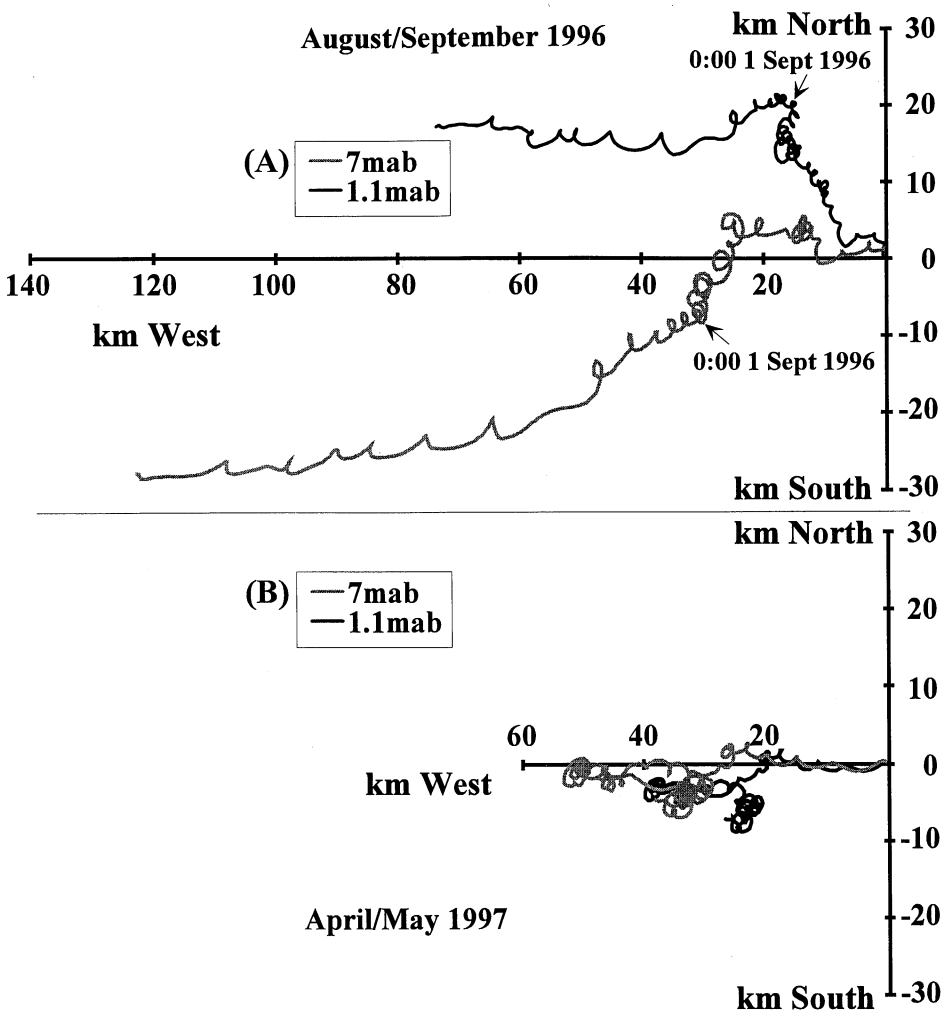

Figure 11. Progressive vector diagrams of currents at 1.1 and 7 m above bottom (mab) from the BASS tripod for (a) summer (September 21 to August 8, 1996) and (b) spring (April 23 to May 13, 1997) at the CMO site.

increased bed shear stress several days before Hurricane Edouard arrived (Plate 4 and Figure 9). Thus we conclude that resuspension of bottom sediments was initially dominated by waves and only later by currents.

At the height of the hurricane, sustained winds exceeded 20 m s^{-1} with 7-8 m waves (Plate 4). The wave shear stress totally dominated the combined wave and current shear stress when the hurricane made closest approach (4 dyn cm^{-2}). We were forced to return to port but arrived back on station about a day after the passage of the hurricane. The winds had decreased to 5 m s^{-1}, but 2 m surface swells were still present. Note that current speeds in bottom waters reached a maximum (35 cm s^{-1}) after the hurricane passed, and the current shear stress became dominant, exceeding 2.3 dyn cm^{-2}. About a day after Hurricane Edouard the nepheloid layer thickness was still 45 m with beam c_p exceeding 2.5 m^{-1} near the bottom (Plate 4c). Bottom PM concentration was fourfold greater than prehurricane values. Two days later, the nepheloid layer was only 20 m thick, and particulate matter concentrations dropped off considerably but were still much greater than prehurricane values.

Young [1978] noted that following a hurricane off the New York Bight apex, particulate matter concentrations in bottom waters were at normal nonhurricane conditions within 3 days. He attributed this rapid clearing to the lack of fine-grained sediment (clay and fine silt) available for resuspension and the fact that the hurricane strength was not sufficient to mix the stratified waters, restricting most of the resuspended sediment to the bottom nepheloid layer. The effects of Hurricane Edouard were much more intense, changing the water column from strong, continuous stratification to a two-layered, weakly stratified system.

Upon our return to the site, solar heating rapidly began to restratify the surface waters, and particle concentrations quickly decreased in bottom waters. The question is whether the particles rapidly flocculated and settled out locally or whether turbid water was replaced with clear water by advection. *Hill et al.* [this issue] observed that large aggregates disappeared from near-bottom waters during the hurricane but quickly reappeared after the hurricane and argued that bottom shear stresses tore the aggregates apart but that lower shear stresses allowed them to reaggregate quickly. While reaggregation could have played an important role in clearing the water of particles, *Chang and Dickey* [this issue] noted that beam c_p decreased simultaneously at all depths at which they had optical sensors on their mooring and bottom tripod at this site (12, 30, 50, and 68 m), suggesting that advection brought

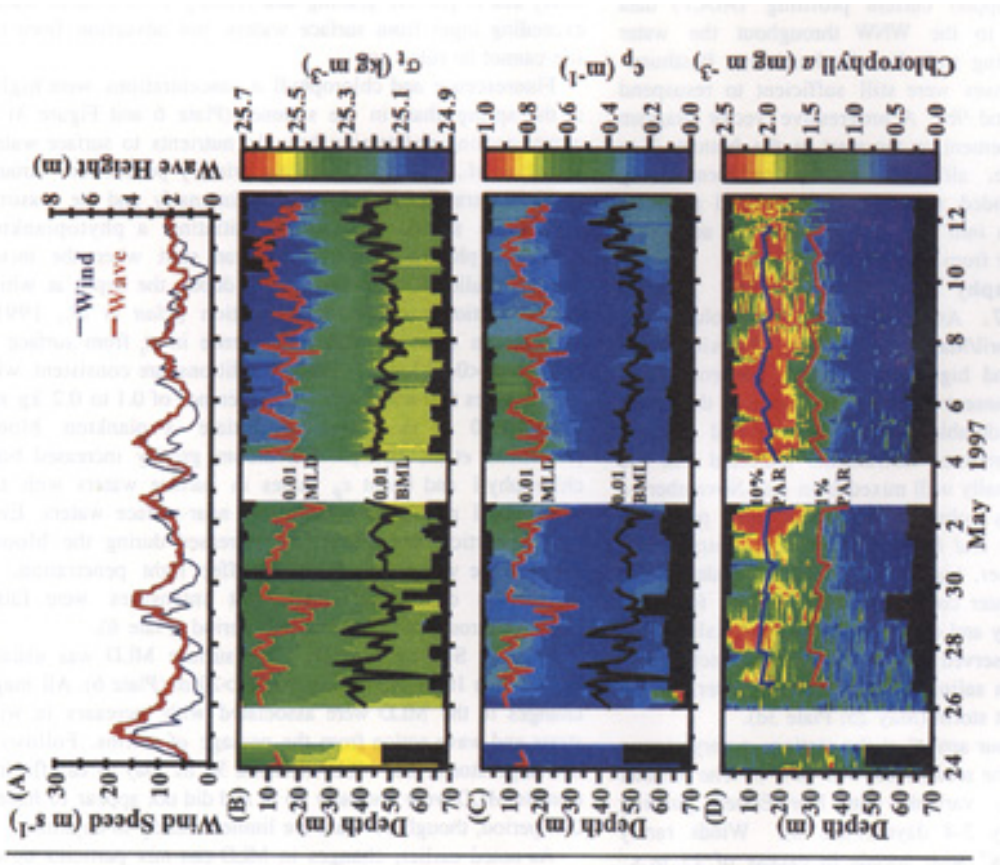

Plate 6. Time series sections of (a) wind speed and wave height (data from S. Anderson et al., WHOI, personal communication, 2000), (b) σ_t, (c) beam c_p, and (d) chlorophyll for the spring 1997 cruise. The 0.01 $\Delta\sigma_t$ MLD (red line) and 0.01 $\Delta\sigma_t$ BML (black line) are plotted on Plates 6b and 6c. The depth of the 10% PAR light depth (blue line) and 1% PAR light depth (red line) are plotted on Plate 6d.

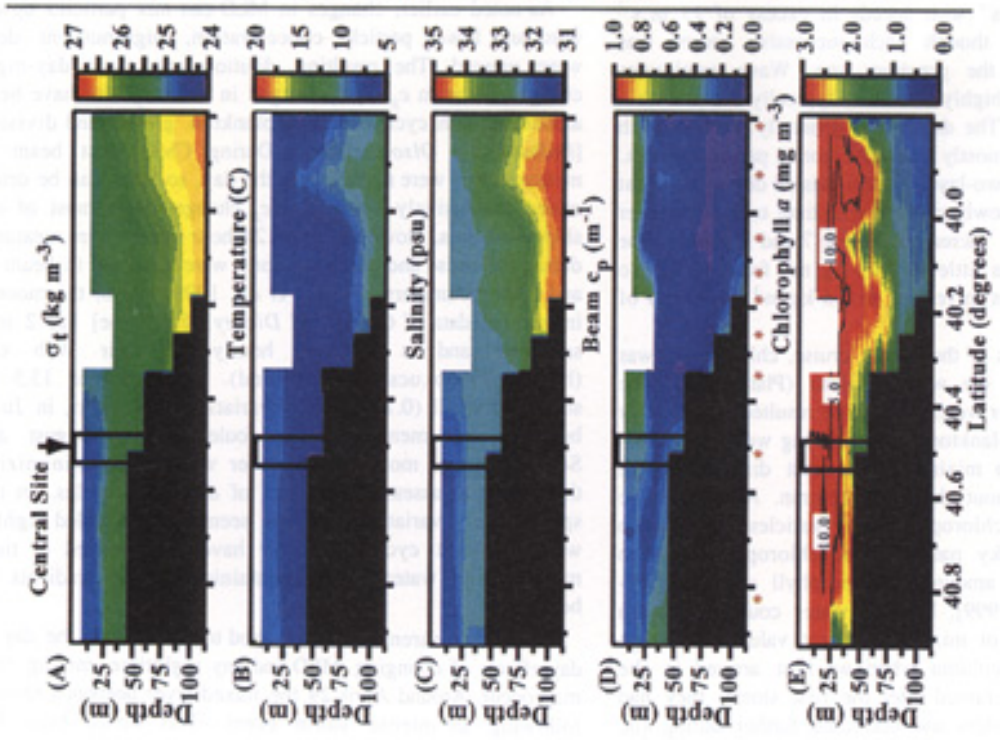

Plate 5. Cross-shelf sections for spring 1997 cruise (May 12-13, 1997). The asterisks below plate 5d indicate station locations.

in clear water rather than particles simply settling out. Indeed, shipboard acoustic Doppler current profiling (ADCP) data revealed strong flow to the WNW throughout the water column, especially during and after the hurricane. Posthurricane bottom shear stresses were still sufficient to resuspend sediment (Figures 9a and 9b). A progressive vector diagram shows rapid water movement to the west in the bottom 7 m (Figure 11). Therefore, although bottom sediments may continue to be resuspended, stratification prevented particles from being carried high into the water column, and advection brought in clearer water from offshore.

3.2.7. Hydrography and atmospheric conditions: Spring 1997. As expected, the water column was weakly stratified in April/May 1997 because of mixing from convective cooling and high winds during frequent winter storms. A cross-shelf transect was made at the end of the cruise after 2 weeks of considerable surface warming had occurred (Plate 5). Data from moored instruments indicated that the water column was thermally well mixed from mid-November to early December but was isohaline for only a short period in early December [*Chang and Dickey*, this issue; *Lentz et al.*, 1999]. In late December, high-salinity water intruded along the bottom, and the water column stratified except for short periods in mid-February and early April. Elevated salinity in bottom water can be observed in data from our transect (Plate 5c). Note the change in salinity throughout the water column before and after the first storm (May 25; Plate 3d).

A few days prior to our arrival at the station, a very strong storm had passed over the area (winds >15 m s^{-1}). The weather continued to be highly variable with Nor'-Easters passing through the area every 3-4 days (Plate 6). Winds rarely dropped below 3-4 m s^{-1} with speeds in excess of 15 m s^{-1} during storm events, though each successive storm was slightly weaker than the previous one. Wave amplitudes during the cruise were highly variable, typically >2 m with a maximum of 4-6 m. The days were generally sunny, with cloudy days occurring mostly when the storms passed through.

A weakly stratified two-layer system existed during the first half of the cruise and slowly evolved with time to a three-layer system as stratification increased (Figure 7 and Plate 6). The σ_t initially varied by as little as 0.05 kg m^{-3} from surface to bottom, with differences increasing to 0.5 kg m^{-3} by the end of the cruise.

During the first days of the spring cruise, chlorophyll was distributed throughout the water column (Plate 6d). The elevated values in deeper waters may have resulted from earlier short periods of phytoplankton blooms during weak stratification followed by deep mixing events that distributed live phytoplankton throughout the water column. An alternative interpretation is that chlorophyll-rich particles settled into deeper waters. The spiky nature of the chlorophyll section suggests a substantial amount of chlorophyll was in aggregates [*Gardner et al.*, 1999], but aggregates could have been introduced by settling or mixing. Nutrient values were high throughout the water column when we first arrived in the spring, but when we returned after the first storm, they had decreased in surface waters and decreased further during the following days [*Sosik et al.*, this issue]. This is consistent with deep mixing events and subsequent biological uptake of nutrients in surface waters. With the onset of stratification (approximately April 29) the chlorophyll concentrations decreased in bottom waters, while they increased in surface waters. The diminished deep-water levels of chlorophyll were likely due to particle grazing and settling from bottom waters exceeding input from surface waters, but advection from the site cannot be ruled out.

Fluorescence and chlorophyll *a* concentrations were higher in the spring than in the summer (Plate 6 and Figure 3) as winter cooling and mixing brought nutrients to surface waters [*Sosik et al.*, this issue], fueling primary production. Around April 29, stratification appeared to intensify and the seasonal pycnocline started to develop, initiating a phytoplankton bloom. A phytoplankton bloom can start when the mixed layer is shallower than the critical depth, the depth at which net production exceeds net respiration [*Platt et al.*, 1991]. This bloom occurred with a difference in σ_t from surface to bottom of <0.20 kg m^{-3}. These conditions are consistent with other studies that noted that a σ_t difference of 0.1 to 0.2 kg m^{-3} over 70-80 m is needed to initiate a plankton bloom [*Townsend et al*, 1992]. The bloom greatly increased both chlorophyll and beam c_p values in surface waters with the chlorophyll maximum occurring in near-surface waters. Even though particle concentrations increased during the bloom, the increase was not sufficient to affect light penetration, as the depths of specific PAR light intensities were fairly constant throughout the sampling period (Plate 6).

3.2.8. Spring MLD. The surface MLD was usually deeper than 10 m and, occasionally, >20 m (Plate 6). All major changes in the MLD were associated with increases in wind stress and wave action from the passage of storms. Following one large storm, the MLD exceeded 30 m. Day to day fluctuations in MLD were normally <5 m and did not appear to have a diel period, though our data are limited mostly to daytime.

As noted earlier, changes in MLD can mix particles downward and lower particle concentration, high-nutrient deep water upward. The resulting dilution can cause day-night changes in beam c_p. Diel changes in beam c_p also have been associated with cycles of phytoplankton growth and division [*DuRand and Olson*, 1996]. During CMO most beam c_p measurements were made during the day, so little can be determined conclusively about diel c_p changes from most of our shipboard data. However, a few 24 hour cycles were measured during the cruise and diel variations were observed in beam c_p and other parameters [*DuRand et al.*, 1999]. Also, the moored instrument data of *Chang and Dickey* [this issue] had 2 min sampling and is averaged hourly on their Web site (http://www.opl.ucsb.edu/cmo.html). Their data at 13.5 m suggest a small (0.1 m^{-1}) daily variation in beam c_p in July, but the instruments became fouled during August and September, and most of September was cloudy, minimizing the ability to assess any impact of diel light cycles. In the spring, daily variations did not seem to be coupled tightly with diel light cycles and may have been related to tidal movement of water masses containing lateral gradients in beam c_p.

Optical measurements can be used to demonstrate the day day effects of changing MLD and any nighttime mixing that may occur. Around April 29 the mixed layer deepened rapidly following an intense storm event. This mixed high PM concentration surface waters with lower PM concentration deeper waters (Figure 8b), increasing beam c_p in the 20-30 m depth range and decreasing beam c_p in surface waters. This process occurred again between May 1 and 3, with two differences. First, there was no clear diel signal. Second, super-

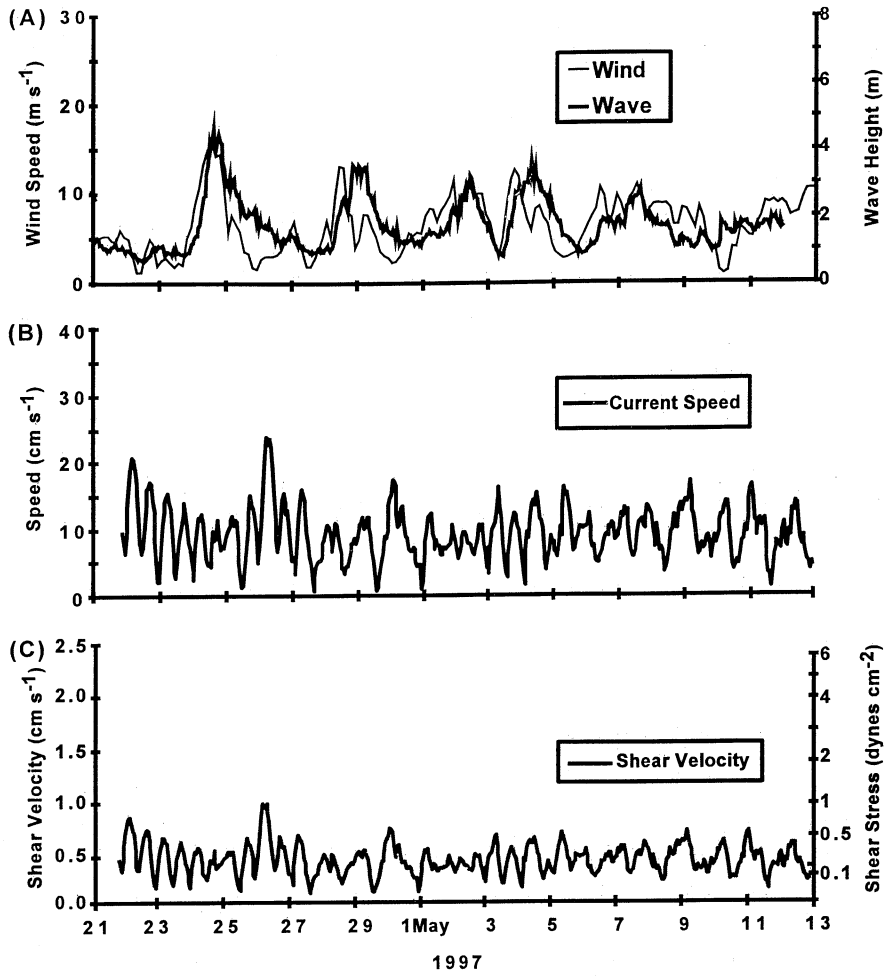

Figure 12. (a) Wind and wave height (data from S. Anderson et al., WHOI, personal communication, 2000), (b) current speed at 1.1 m above bottom (data from A. Williams et al., personal communication, 2000), and (c) shear velocities calculated from currents at 0.74 m above bottom during the spring 1997 cruise. Wave shear velocity data were not available for this period.

imposed on the second mixing event was the initiation of a plankton bloom, which would tend to increase beam c_p and negate the decreases caused by dilution.

3.2.9. Near-bottom currents and shear stress: Spring 1997. The BML was slightly thicker in spring (20-30 m) than in summer (10-20 m). Beam c_p generally decreased at the top of the BML, so both hydrography and optics could be used to mark the boundary between middle and bottom waters. Distinguishing between middle and bottom waters on the basis of bulk composition of particles was not very definitive as the particles were a mix from surface and bottom sources (Figures 2-5).

Beam c_p and particle concentrations in the nepheloid layer were low during much of the spring period (Figure 7 and Plate 6), but there were brief periods of increased concentration that appeared to be associated with surface storms. Peaks in the bottom current speed occurred 1-2 days after the peak in wind speed and wave height (Figure 12). Unfortunately, the instruments used in the summer to measure wave shear velocity were not deployed in the spring, so we cannot be sure of the periods of maximum combined wave and current shear. Beam c_p increased near the bottom when storms passed by, but the gaps in our profiling data made it difficult to show correlations as clearly as with moored instruments. Rough weather also made it more difficult to profile to a consistent height above bottom, and changes can happen rapidly. For example, beam c_p was only 0.5 m^{-1} with no near-bottom increase down to 68 m on one cast, yet it increased from 1.5 to 5.5 m^{-1} between 67.5 and 69.5 m 9 hours later. Fluorescence also doubled in that interval, suggesting rapid resuspension of fresh phytodetritus. The next CTD cast an hour later went to only 58 m, failing to collect any near-bottom data. The moored data of *Chang and Dickey* [this issue] indicated a doubling of beam c_p at 68 m depth during the storms of April 25 and 29 but not the factor of 4 increase noted in the single CTD profile, suggesting resuspension can vary significantly over short distances in the area.

Beam c_p increased during the last 3 days of the cruise, even though there was no significant increase in wind, waves, or currents. Salinity increased simultaneously with increases in beam c_p, suggesting that the increases were due to advection of turbid water rather than to local resuspension. This is consistent with the moored data of *Chang and Dickey* [this issue].

3.2.10. Intrusions summer/spring. *Palanques and Biscaye* [1992] noted that intrusions of slope water onto the shelf could rapidly change the vertical profile of particle

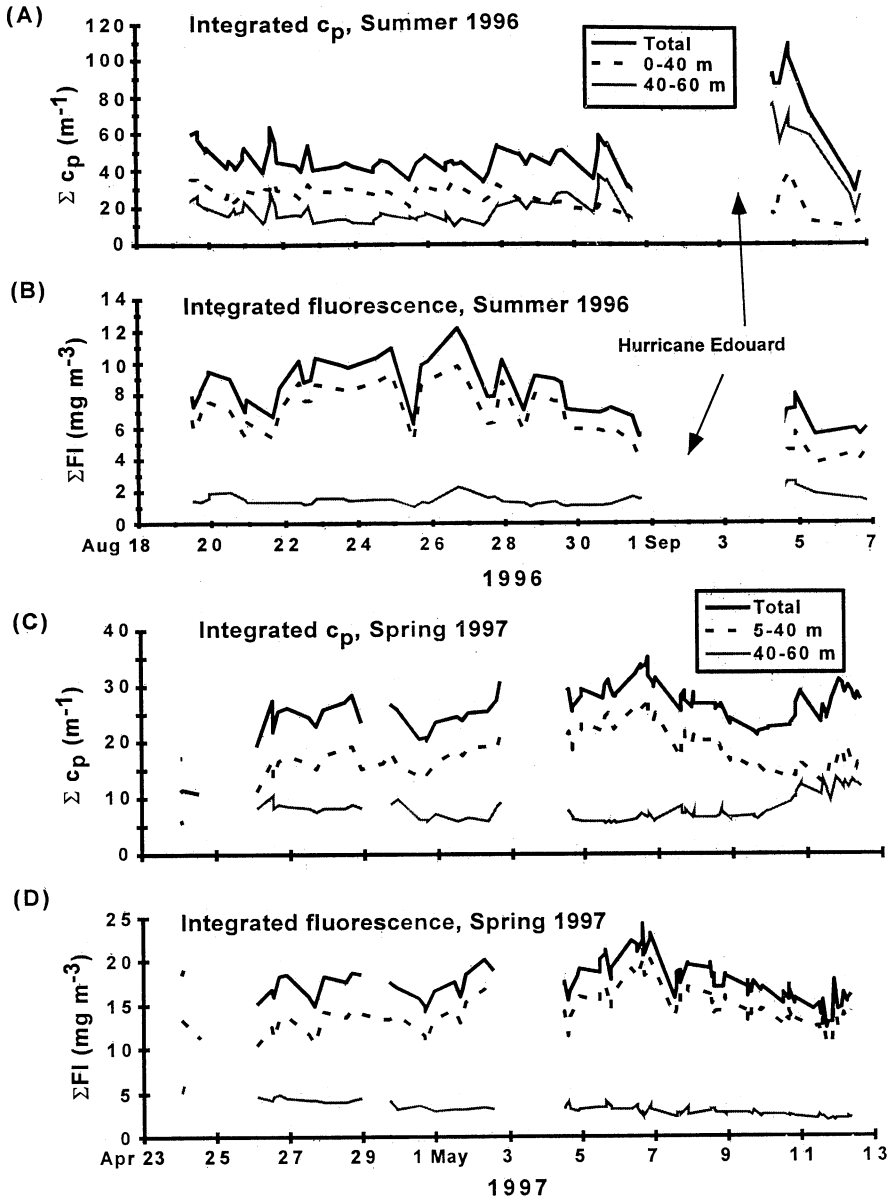

Figure 13. Integrated (a) beam c_p and (b) fluorescence over given depth intervals and the whole water column for the summer 1996 cruise (c) beam c_p and (d) fluorescence for the spring 1997 cruise.

concentration at a given location independent of particle settling or resuspension. Subsurface intrusions are not visible from satellite observations but were often apparent in sections made by rapid sampling with an undulating profiler [*Barth et al.*, 1998; W. S. Pegau et al., Mixing of optical properties as evidenced in salinity intrusions observed during the Coastal Mixing and Optics Experiment, submitted to *Journal of Geophysical Research*, 2000, hereinafter referred to as Pegau et al., submitted manuscript, 2000].

Subsurface intrusions entered the CMO site during the summer and spring cruises (Pegau et al., submitted manuscript, 2000). On August 25 a high-salinity intrusion entered the central CMO site from continental slope waters at about 10-25 m (Plate 3). The intrusion of higher-salinity water appears to have pushed the existing water mass deeper as the PM and chlorophyll maxima, along with the associated 24.6 isopycnal, moved ~10 m deeper (Plates 3 and 4). Following this intrusion, a brief bloom occurred in the waters beneath the intrusion, creating the highest chlorophyll values measured during the cruise (August 26). Measurements of particle size in the high particle concentration waters showed a shift from large to small particles [*Blakey*, 1999]. On the basis of moored measurements of inherent optical properties, a shift in species composition also occurred at this time [*Chang and Dickey*, 1999].

A second, less obvious intrusion entered the site in the surface waters several days prior to the hurricane (August 30), again bringing in offshore waters [*Chang and Dickey*, this issue]. Temperature remained constant, but salinity increased slightly (Plate 3). Chlorophyll values decreased rapidly throughout the surface layer, and the subsurface maximum weakened. Maximum particle concentrations shifted toward the surface (Plate 4). *Sosik et al.* [this issue] noted a deepening of the low-nutrient values at this time and argued that the lower

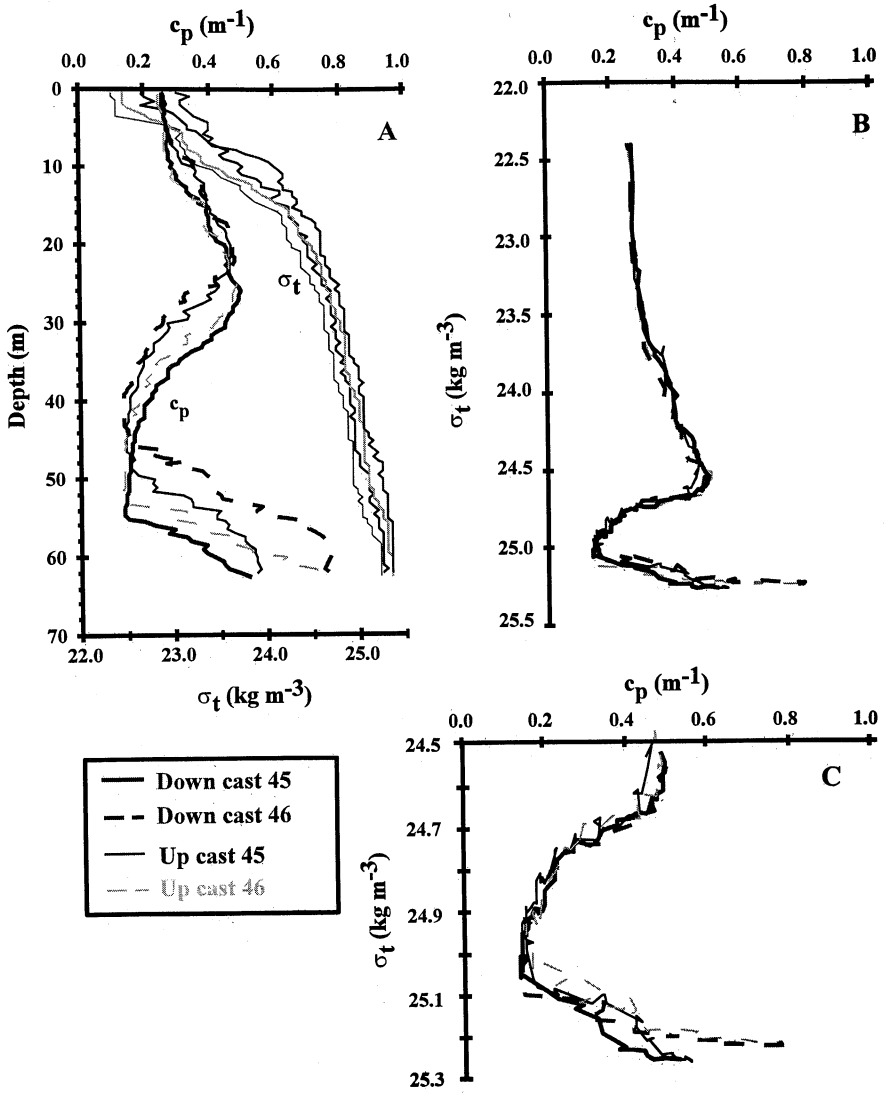

Figure 14. Examples of the effects of internal waves during August 1996 from two casts taken 30 min apart. When beam c_p is plotted as (a) a function of depth, each trace is different, but when plotted as (b) a function of σ_t, the traces are nearly identical. The slight difference seen in (c) the expansion of the lower water column reveals changes in beam c_p that result from resuspension and/or advection.

chlorophyll values resulted from advection of water with different properties. Other possible, but less likely explanations, for the changes in the upper water column particle and pigment distributions are (1) a decrease in production or (2) an increase in grazing and/or aggregation. Increased rates of vertical mixing alone cannot explain the decrease in the integrated particle load (Figure 13), however, increased mixing could decrease production by lowering average light exposure and disrupting the light adaptation of the existing phytoplankton species.

The only major surface intrusion during the spring cruise occurred beginning on May 8 when fresher water entered the site in the upper 20-25 m and was present for the remainder of the cruise (Plates 3 and 6). The intrusion also brought in water with lower values of beam c_p and lower chlorophyll concentrations (Plate 6). Initially, it appeared that the decrease in chlorophyll meant the bloom was ending, but upon further analysis it was seen that phytoplankton cell concentrations continued to increase while the composition shifted toward smaller and less pigmented cells [*Sosik et al.*, 1998, this issue]. Measurements of particle size showed a major shift from 10-16 μm particles to particles in the 2-3 and 8-10 μm size range [*Blakey*, 1999].

3.2.11. Internal waves and solitons: Comparison of summer and spring. The mean current speed calculated from the BASS current data for the first 11 days of the summer cruise (August 20-31) was 8.7 cm s^{-1} compared with 9.4 cm s^{-1} for the whole spring cruise (Figures 9 and 12). Mean bed shear velocity [*Chang et al.*, this issue] was slightly larger in the spring (0.39 versus 0.36 cm s^{-1}), yet beam attenuation (and particle concentrations) in the bottom nepheloid layer was 50-100% greater in the summer (Figures 2 and 4 and Plates 4 and 6). On the basis of current shear velocity, there were more periods when critical shear velocity was exceeded in spring than in summer (prior to the hurricane). What factors would cause higher concentrations when mean shear velocities were lower?

Several studies have identified internal waves as being

responsible for increased resuspension of bottom sediments [*Young et al.*, 1981; *Cacchione and Drake*, 1986; *Bogucki et al.*, 1997; *Wang et al.*, this issue]. Internal waves are more common and intense during summer months when shelf water is strongly stratified, so more sediment could be resuspended during summer than during spring [*Butman and Folger*, 1979] and may explain the difference.

We were able to observe the effects of large internal waves during CTD casts when temperature and salinity were offset by as much as 10 m in <30 min (Figure 14). When properties such as beam c_p were plotted by depth, a definitive offset was seen in closely timed successive casts. When plotted versus σ_t, the beam c_p profiles lay nearly on top of one another, suggesting that water with the same physical and optical properties was moving up and down in the water column. Looking in detail at the near-bottom region, the passage of the internal waves coincides with an increase in beam c_p, suggesting that internal waves caused resuspension at this site (Figure 14).

In addition to internal waves, solitons were identified passing the moored CMO current meters [*Boyd et al.*, 1997; *Chang and Dickey*, this issue] during the summer cruise. Passage of solitons could be observed in real time as large perturbations in the velocity structure and particle concentrations (based on backscatter) within the water column from the ADCP data. Their passage was also noted visually in the characteristic changes in sea surface roughness [*Porter et al.*, this issue]. Although there was at least one occasion when we had the CTD in the water during the passage of a soliton, our profiling rate was too slow to characterize or quantify the influence of the passage of solitons, which traveled past the ship in <15 min. J. MacKinnon and M. Gregg (Mixing on the late-summer New England shelf: Solibores and stratification, submitted to *Journal of Geophysical Research*, 2000) have examined the effects of internal waves and solitons during the summer.

While the difference in resuspension intensity between the fall and spring cruises may result largely from the difference in internal wave and soliton activity, there are additional potential factors, such as a change in sediment cohesion. *Butman and Folger* [1979] and *Butman et al.* [1979] also reported seasonal changes in resuspension off the mid-Atlantic continental shelf. They found that during the winter, bacterial mats formed on the sediment surface, making it more difficult to initiate resuspension. The cores we took during the spring had what appeared to be a cohesive surface mat or gel, but no bacterial analyses were made.

4. Summary and Conclusions

The extreme conditions of (1) low stratification during the spring onset of warming punctuated with frequent storms and (2) the highly stratified summer period punctuated with the passage of Hurricane Edouard provided an ideal setting for comparing bulk particle characteristics and optical signals under a wide range of physical mixing conditions and biological productivity.

On the basis of hydrography and optics the spring water column was a weakly stratified two-layer system that developed into a three-layer system early in the cruise and probably persisted through the summer. Changes in hydrographic parameters (T, S, and σ_t) were usually matched by changes in optical parameters (c_p, LSS, and Fl), e.g., at the base of the surface mixed layer and at the top of the BML. The boundary of the surface layer corresponds with the base of the chlorophyll layer (not the MLD). The boundary of the bottom layer corresponded with the top of the bottom nepheloid layer, which usually corresponded with the BML. The optical characteristics of particles in surface waters varied significantly between summer and spring (Figures 2-5). However, during both time periods, particles in surface waters were primarily biological in origin. Property-property plots of bulk particle (POC, PM, and chlorophyll) and optical (beam c_p and scattering) parameters provide more information for identifying layers with different particle types than optical profiles alone. Particles in surface layers were distinctly different from those in bottom waters in most property-property plots but not in others. In midwaters the particle/optical parameters overlapped with particles in surface or bottom layers, depending on the time of year and mixing history, because particles in this region may have come from either the surface via settling or the bottom from resuspension. The use of multiple compositional or optical parameters makes the identification of different layers more reliable. For example, beam c_p was well correlated with PM in surface and bottom layers, but the beam c_p:PM ratio differed by a factor of 3 for different layers and times, making it impossible to predict particle concentration without taking some bulk water samples. POC concentrations were even less predictable because of multiple sources of particle types. The various ratios involving c_p or LSS depend on both the index of refraction of the particles and their size distribution. Other parameters such as POC/PM tell us nothing about size distribution but are an indication of the expected index of refraction of the particles (organic matter has a lower index of refraction than nonbiogenic particles). The combination of parameters can thus be used to assess at least qualitatively both index of refraction and particle size distribution (Twardowski et al., submitted manuscript, 2000).

In the summer the resuspended sediment was generally confined to the BML until prehurricane surface swells and the passage of Hurricane Edouard resuspended large amounts of surface sediment and transformed the water column from well-stratified to a weakly stratified, two-layer mixed system. Particle concentrations decreased rapidly throughout the water column after the hurricane passed, but this appears to be due to advection more than to local particle settling. On the basis of optical and bulk particle parameters (Figures 2-5), there was also a change in the bulk composition and optical properties of particles throughout the water column before and after the hurricane as well as between summer and spring.

The concentration of particulate material in the upper 40 m of the water was roughly comparable in spring and summer (prehurricane), whereas the bottom 20 m contained at least twice as much particulate matter in summer than in spring, presumably because of more active resuspension. Chlorophyll concentrations were 2-3 times higher in spring because of bloom conditions. Maximum chlorophyll (and beam c_p) was in surface waters in spring but formed a subsurface maximum in summer. Chlorophyll was more evenly distributed throughout the entire water column during the first portion of the cruise (Plate 6). As stratification increased, the chlorophyll levels in the deeper waters declined considerably.

The mooring data [*Chang and Dickey*, this issue] suggested that the hurricane nearly mixed the water column top to bottom, but by the time our ship returned 2 days after the hurricane, there was a weak two-layer system, with each layer still fairly well mixed (Plate 4). Surface temperature dropped >6°C, and the subsurface chlorophyll maximum nearly disappeared. However, 2 days after the hurricane, the MLDs

were the same as they were prior to the hurricane, evidence of rapid posthurricane restratification (Plate 4 and Figure 8). In contrast, stratification in the spring was very weak, so winds of similar magnitude during the spring storms deepened the surface mixed layer, which quickly shoaled after the storm passed and solar heating stratified surface waters. The depth of mixing decreased as the seasonal pycnocline developed.

Although the local winds were of similar magnitude during the hurricane and spring storms, the wave height was nearly 50% larger during the hurricane than during spring storms. The degree of bottom resuspension was substantially less during spring storms than during the hurricane (Plates 4 and 6). Bottom currents and shear stress increased after the spring storms passed, but no wave shear stress measurements were obtained during that period for comparison with the hurricane period. The increased shear appears to have caused brief periods of resuspension during the spring storms, but the increases in PM were generally small and confined near bottom compared with resuspension during the hurricane. We suggest the difference was related to the longer-period waves during the hurricane, which generated very large bed shear stresses and were later dominated by current shear stress. The presence of bacterial mats binding surface sediments may have been partially responsible for the lower degree of resuspension in the spring.

If we can extrapolate an annual cycle from these two data sets, it appears that during the winter, resuspended sediment could be spread throughout the water column [Orr and Hess, 1978] and remaining biogenic particles could be similarly distributed. With the onset of stratification the sources of particles in the surface layer were primarily biogenic. Resuspended particles that are mixed upward may bring particulate matter into the middle water, during which times the composition of particles would be similar to those in bottom waters. Further stratification inhibits the upward mixing. Without resuspension the only source of particles in middle water is from biogenic particles settling from surface waters, so the optical properties tend toward those in surface waters. However, particle and optical properties change as particles are consumed, recycle, aggregate, and settle. While particles are not conservative, they are useful tracers of short-term events. Their distribution can be determined rapidly with optical instruments, but measurements of bulk particle properties aid significantly in defining layers of particles of similar origin, which result from the combined effects of biology, physical forcing, and particle dynamics.

Acknowledgments. We thank our many colleagues in the Coastal Mixing and Optics program and the captains and shipmates on the R/V *Seward Johnson* and the R/V *Knorr* for their help, collaboration, and stimulating discussions during the cruises and workshops of this program. We thank Tommy Dickey and Grace Chang for their moored instrument data and George Voulgaris and Grace Chang for their current and wave bed shear calculations. The assistance of Jan Gundersen, Sarah Searson, and Chris Nugent is appreciated in collecting and presenting the data. The comments of three anonymous reviewers and Tommy Dickey were very helpful in focusing the results. We thank Joseph Kravitz, Steven Ackleson, Lou Goodman, and Tom Kinder for support and encouragement during this program. This work was funded by ONR contract N000014-95-1-0498.

References

Armi, L., Mixing in the deep ocean: The importance of boundaries, *Oceanus, 21*, 14-19, 1978.

Armi, L., and E. D'Asaro, Flow structures of the benthic ocean, *J. Geophys. Res., 85*, 469-484, 1980.

Baker, E. T., and J. W. Lavelle, The effect of particle size on the light attenuation coefficient of natural suspensions, *J. Geophys. Res., 89*, 8198-8203, 1984.

Barth, J. A., D. Bogucki, S. D. Pierce, and P. M. Kosro, Secondary circulation associated with a shelfbreak front, *Geophys. Res. Lett., 25*, 2761-2764, 1998.

Bartz, R., R. J. V. Zaneveld, and H. Pak, Transmission for profiling and moored observation in water, in *Ocean Optics V*, edited by M. B. White, pp. 102-108, Int. Soc. for Opt. Eng., Bellingham, Wash., 1978.

Beardsley, R. C., and B. Butman, Circulation on the New England continental shelf: Response to strong winter storms, *Geophys. Res. Lett., 1*, 181-184, 1974.

Bishop, J. K. B., The correction and suspended particulate matter calibration of Sea Tech transmissometer data, *Deep Sea Res., Part A, 33*, 121-134, 1986.

Blakey, J., The distribution and optical response of particles on the continental shelf and their relationship to cross-isopycnal mixing, M.S. thesis, Texas A&M Univ., College Station, 1999.

Bogucki, D., T. Dickey, and L. G. Redekopp, Sediment resuspension and mixing by resonantly generated internal solitary waves, *J. Phys. Oceanogr., 27*, 99-114, 1997.

Bothner, M. H., C. M. Parmenter, and J. D. Milliman, Temporal and spatial variations in suspended matter in continental shelf slope waters off the north-eastern United States, *Estuarine Coastal Shelf Sci., 13*, 213-234, 1981.

Boyd, T., M. D. Levine, and S. R. Gard, Mooring observations from the Mid-Atlantic Bight, *Rep. 97-2-164*, 226 pp., Oregon State Univ., Corvallis, 1997.

Brainerd, K. E., and M. C. Gregg, Surface mixed layer and mixing layer depths, *Deep Sea Res., Part I, 42*, 1521-1543, 1995.

Bricaud, A., A. Morel, and L. Prieur, Absorption by dissolved organic matter of the sea (yellow substance) in the UV and visible domains, *Limnol. Oceanogr., 26*, 43-53, 1981.

Bumpus, D. F., and L. M. Lauzier, Surface circulation on the continental shelf of eastern North America between Newfoundland and Florida, American Geographical Society, in *Serial Atlas of the Marine Environment*, folio 7, 4 pp., Am. Geogr. Soc., New York, 1965.

Bunt, J. A. C., P. Larcombe, and C. F. Jago, Quantifying the response of optical backscatter devices and transmissometers to variations in suspended particulate matter, *Cont. Shelf Res., 19*, 1199-120, 1999.

Butman, B., Physical processes causing surficial sediment movement, in *Georges Bank*, edited by R. Backus, pp. 147-162, MIT Press, Cambridge, Mass., 1987.

Butman, B., and D. W. Folger, An instrument system for long-term sediment transport studies on the continental shelf, *J. Geophys. Res., 84*, 1215-1220, 1979.

Butman, B., and M. Nobel, Long term in situ observations of bottom sediment movement on the U.S. Atlantic continental shelf (abstract), *Eos Trans. AGU, 59*, 295, 1978.

Butman, B., M. Nobel, and D. W. Folger, Long-term observations of bottom current and bottom sediment movement on the Mid-Atlantic continental shelf, *J. Geophys. Res., 84*, 1187-1205, 1979.

Butman, B., R. C. Beardsley, B. Magnell, D. Frye, J. A. Vermersch, R. Schlitz, R. Limeburner, W. R. Wright, and M. A. Nobel, Recent observations of the mean circulation on Georges Bank, *J. Phys. Oceanogr., 12*, 569-591, 1982.

Cacchione, D. A., and D. E. Drake, Nepheloid layers and internal waves over continental shelves and slopes, *Geo Mar. Lett., 6*, 147-152, 1986.

Chang, G. C., and T. D. Dickey, Partitioning in situ total spectral absorption by use of moored spectral absorption-attenuation meters, *Appl. Opt., 38*, 3876-3887, 1999.

Chang, G. C., and T. D. Dickey, Optical and physical variability on timescales from minutes to the seasonal cycle on the New England continental shelf: July 1996 to June 1997, *J. Geophys. Res.*, this issue.

Chang, G. C., T. D. Dickey, and A. J. Williams III, Sediment resuspension over a continental shelf during Hurricanes Edouard and Hortense, *J. Geophys. Res.*, this issue.

Christoffersen, J. B., and I. G. Jonnson, Bed friction and dissipation in a combined current and wave motion, *Ocean Eng., 12*, 387-423, 1985.

Chung, S. P., W. D. Gardner, M. J. Richardson, I. D. Walsh, and M. R. Landry, Beam attenuation and micro-organisms: Spatial and temporal variations in small particles along 140°W during the 1992 JGOFS EqPac transects, *Deep Sea Res., Part II, 43*, 1205-1226, 1996.

Chung, S. P., W. D. Gardner, M. R. Landry, M. J. Richardson, and I. D.

Walsh, Beam attenuation of microorganisms and detrital particles in the equatorial Pacific, *J. Geophys. Res., 103*, 12,669-12,681, 1998.

Claustre, H., A. Morel, M. Babin, C. Cailliau, D. Marie, J.-C. Marty, D. Tailliez, and D. Vaulot, Variability in particle attenuation and chlorophyll fluorescence in the tropical Pacific: Scales, patterns, and biogeochemical implications, *J. Geophys. Res., 104*, 3401-4322, 1998.

Conner, C. S., and A. M. De Visser, A laboratory investigation of particle size effects on an optical backscatterance sensor, *Mar. Geol., 108*, 151-159, 1992.

Dickey, T. D., and A. J. Williams III, Interdisciplinary ocean process studies on the New England shelf, *J. Geophys. Res.*, this issue.

Dickey, T. D., G. C. Chang, Y. C. Agrawal, A. J. Williams III, and P. S. Hill, Sediment resuspension in the wakes of Hurricanes Edouard and Hortense, *Geophys. Res. Lett., 25*, 3533-3536, 1998.

DuRand, M., and R. J. Olson, Contributions of phytoplankton light scattering and cell concentration changes to diel variations in beam attenuation in the equatorial Pacific from flow cytometric measurements of pico-, ultra-, and nanoplankton, *Deep Sea Res., Part II, 43*, 891-906, 1996.

DuRand, M. D., H. M. Sosik, and R. J. Olson, Diel variations in single-cell and bulk optical properties during the Coastal Mixing and Optics experiment (abstract), *Eos Trans. AGU*, 80(49), Ocean Sci. Meet. Suppl., OS26, 1999.

Flagg, C. N., Hydrographic structure and variability, in *Georges Bank*, edited by R. Backus, pp. 108-124, MIT Press, Cambridge, Mass., 1987.

Gardner, W. D., Baltimore Canyon as a modern conduit of sediment to the deep sea, *Deep Sea Res., Part A, 36*, 323-358, 1989.

Gardner, W. D., P. E. Biscaye, R. V. Zaneveld, and M. J. Richardson, Calibration and comparison of the LDGO nephelometer and the OSU transmissometer on the Nova Scotian Rise, *Mar. Geol., 66*, 323-344, 1985.

Gardner, W. D., I. D. Walsh, and M. J. Richardson, Biophysical forcing of particle production and distribution during a spring bloom in the North Atlantic, *Deep Sea Res., Part II, 40*, 171-195, 1993.

Gardner, W. D., S. P. Chung, M. J. Richardson, and I. D. Walsh, The oceanic mixed-layer pump, *Deep Sea Res., Part II, 42*, 757-775, 1995.

Gardner, W. D., J. S. Gundersen, M. J. Richardson, and I. D. Walsh, The role of diel variations in mixed-layer depth on the distribution, variation, and export of carbon and chlorophyll in the Arabian Sea, *Deep Sea Res., Part II, 46*, 1833-1858, 1999.

Grant, W. D., and O. S. Madsen, Combined wave and current interaction with a rough bottom, *J. Geophys. Res., 84*, 1797-1808, 1979.

Hall, I. R., S. Schmidt, I. N. McCave, and J. L. Reyss, Particulate matter distribution and $^{234}Th/^{238}U$ disequilibrium along the Northern Iberian Margin: Implications for particulate organic carbon export, *Deep Sea Res., Part I, 47*, 557-582, 2000.

Haury, L. R., P. H. Wiebe, M. H. Orr, and M. G. Briscoe, Tidally generated high-frequency internal wave-packets and their effects on plankton in Massachusetts Bay, *J. Mar. Res., 41*, 65-112, 1983.

Hill, P. S., G. Voulgaris, and J. H. Trowbridge, Controls on floc size in a continental shelf bottom boundary layer, *J. Geophys. Res.*, this issue.

Hobson, L. A., and C. J. Lorenzen, Relationships of chlorophyll maxima to density structure in the Atlantic Ocean and Gulf of Mexico, *Deep Sea Res. Oceanog. Abstr., 19*, 297-306, 1972.

Houghton, R. W., R. Schlitz, R. C. Beardsley, B. Butman, and J. L. Chamberlin, The Middle Atlantic Bight cold pool: Evolution of the temperature structure during summer 1979, *J. Phys. Oceanogr., 12*, 1019-1029, 1982.

Iturriaga, R., A. Morel, C. Roesler, and D. Stramski, Individual and bulk analysis of the optical properties of marine particulates: examples of merging these two scales of analysis, in *Particle Analysis in Oceanography, NATO ASI Ser. G*, vol. 27, edited by S. Demers, pp. 339-347, Springer-Verlag, New York, 1991.

Jerlov, N. G., *Marine Optics*, 231 pp., Elsevier Sci., New York, 1976.

Kitchen, J. C., and J. R. V. Zaneveld, On the noncorrelation of the vertical structure of light scattering and chlorophyll *a* in case I waters, *J. Geophys. Res., 95*, 20,237-20,246, 1990.

Lentz, S., A. Plueddemann, S. Anderson, and J. Edson, Current variability on the New England shelf during the Coastal Mixing and Optics Program, August 1996 - June 1997, *Eos Trans. AGU, 80*(49), Ocean Sci. Meet. Suppl., OS24, 1999.

Loder, J. W., and D. A. Greenberg, Predicted positions of tidal fronts in the Gulf of Maine region, *Cont. Shelf Res., 6*, 397-414, 1986.

Manheim, F. T., R. H. Meade, and G. C. Bond, Suspended matter in surface waters of the Atlantic continental margin from Cape Cod to the Florida Keys, *Science, 167*, 371-376, 1970.

Marra, J., Analysis of diel variability in chlorophyll fluorescence, *J. Mar. Res., 55*, 767-784, 1997.

Mayer, D. A., D. V. Hansen, and D. A. Ortman, Long-term current and temperature observations on the middle Atlantic shelf, *J. Geophys. Res., 84*, 1776-1792, 1979.

Meade, R. H., P. L. Sachs, F. T. Manheim, J. C. Hathaway, and D. W. Spencer, Sources of suspended matter in the waters of the Middle Atlantic Bight, *J. Sediment. Petrol., 75*, 171-185, 1975.

Miller, M. C., N. McCave, and P. D. Komar, Threshold of sediment motion under unidirectional currents, *Sedimentology, 24*, 507-527, 1977.

Moody, J. A., B. Butman, and M. H. Bothner, Near-bottom suspended matter concentration on the continental shelf during storms estimates based on in situ observations of light transmission and a particle size dependent transmissometer calibration, *Cont. Shelf Res., 7*, 609-628, 1987.

Morel, A., Optics of marine particles and marine optics, Individual and bulk analysis of the optical properties of marine particulates: Examples of merging these two scales of analysis, in *Particle Analysis in Oceanography, NATO ASI Ser. G*, vol. 27, edited by S. Demers, pp. 141-188, Springer-Verlag, New York, 1991.

Orr, M. H., and F. R. Hess, Remote acoustic monitoring of natural suspensate distributions, active suspensate resuspension, and slope/shelf water intrusions, *J. Geophys. Res., 83*, 4062-4068, 1978.

Orr, M. H., L. R. Haury, P. H. Wiebe, and M. G. Briscoe, Backscatter of high-frequency (200 kHz) acoustic wavefields from ocean turbulence, *J. Acoust. Soc. Am., 108*, 1595-1601, 2000.

Pak, H., and V. Zaneveld, Bottom nepheloid layers and bottom mixed layers observed on the continental shelf off Oregon, *J. Phys. Oceanogr., 82*, 3921-3931, 1977.

Pak, H., D. A. Kiefer, and J. C. Kitchen, Meridional variations in the concentration of chlorophyll and microparticles in the North Pacific Ocean, *Deep Sea Res., Part A, 35*, 1151-1171, 1988.

Palanques, A., and P. E. Biscaye, Patterns and controls of the suspended matter distribution over the shelf and upper slope south of New England, *Cont. Shelf Res., 12*, 577-600, 1992.

Platt, T., D. F. Bird, and S. Sathyendranath, Critical depth and marine primary production, *Proc. R. Soc. London, Ser. B, 246*, 205-217, 1991.

Porter, D. L., D. R. Thompson, W. Alpers, and R. Romeiser, Remotely sensed ocean observations of the Coastal Mixing and Optics site from synthetic aperture radars and advanced very high resolution radiometers, *J. Geophys. Res.*, this issue.

Price, J. F., and R. A. Weller, Diurnal cycling: Observations and models of the upper ocean response to diurnal heating, cooling, and wind mixing, *J. Geophys. Res., 91*, 8411-8427, 1986.

Richardson, M. J., Particle size, light scattering and composition of suspended matter in the North Atlantic, *Deep Sea Res., Part A, 34*, 1301-1329, 1987.

Ryan, J. P., J. A. Yoder, J. A. Barth, and P. C. Cornillon, Chlorophyll enhancement and mixing associated with meanders of the shelf break front in the Mid-Atlantic Bight, *J. Geophy. Res., 104*, 23,479-23,493, 1999.

Sandstrom, H., and J. A. Elliott, Internal tide and solitons on the Scotian Shelf: A nutrient pump at work, *J. Geophys. Res., 89*, 6415-6426, 1984.

Siegel, D. A., T. D. Dickey, L. Washburn, M. K. Hamilton, and B. G. Mitchell, Optical determination of particulate abundance and production variations in the oligotrophic ocean, *Deep Sea Res., Part A, 36*, 211-222, 1989.

Sosik, H. M., R. E. Green, and R. J. Olson, Optical variability in coastal waters of the Northwest Atlantic, in *Ocean Optics XIV*, edited by S. G. Ackleson, pp. 1-14, Int. Soc. for Opt. Eng., Bellingham, Wash., 1998.

Sosik, H. M., R. E. Green, W. S. Pegau, and C. S. Roesler, Temporal and vertical variability in optical properties of New England shelf waters during late summer and spring, *J. Geophys. Res.*, this issue.

Spinrad, R. W., A calibration diagram of specific beam attenuation, *J. Geophys. Res., 91*, 7761-7764, 1986.

Tandon, A., and C. Garrett, On a recent parameterization of mesoscale eddies, *J. Phys. Oceanogr., 26*, 406-411, 1996.

Townsend, D. W., M. D. Keller, M. E. Sieracki, and S. G. Ackleson, Spring phytoplankton blooms in the absence of vertical water column stratification, *Nature, 360*, 59-62, 1992.

Twitchell, D. C., C. E. McClennen, and B. Butman, Morphology and processes associated with the accumulation of the fine-grained sediment deposit on the southern New England shelf, *J. Sediment. Petrol., 51*, 269-280, 1981.

van Rijn, L. C., Sediment transport, part II, Suspended load transport, *J. Hydraul. Eng., 110*, 1613-1641, 1984.

Wang, B., D. J. Bogucki, and L. G. Redekopp, Particle motions and distributions resulting from the action of solitary waves, *J. Geophys. Res.*, this issue.

Weller, R. A., Observations of the velocity response to wind forcing in the upper ocean, *J. Geophys. Res., 86*, 1969-1977, 1981.

Young, R. A., Suspended-matter distribution in the New York Bight apex related to Hurricane Belle, *Geology, 6*, 301-304, 1978.

Young, R. A., T. L. Clarke, R. Mann, and D. J. P. Swift, Temporal variability of suspended particulate concentrations in the New York Bight, *J. Sediment. Petrol., 51*, 293-306, 1981.

Zaneveld, J. R. V., Variation of optical sea water parameters with depth, in *Optics of the Sea: Interface and In-Water Transmission and Imagery, AGARD-NATO Lecture Ser. 61*, pp. 2.3-1-2.3-22, Advis. Group for Aerospace Res. and Dev., North Atlantic Treaty Org., Brussels, 1973.

Zaneveld, J. R. V., J. C. Kitchen, and H. Pak, Effect of particle size distribution and chlorophyll content on beam attenuation spectra, *Appl. Opt., 21*, 3913-3918, 1982.

J. C. Blakey, W. D. Gardner, and M. J. Richardson, Department of Oceanography, Texas A&M University, College Station, TX 77843-3146. (wgardner@ocean.tamu.edu)

M. C. Gregg and J. A. MacKinnon, Applied Physics Laboratory and School of Oceanography, University of Washington, Seattle, WA 98105.

S. Pegau, I. D. Walsh, and J. R. V. Zaneveld, College of Oceanic and Atmospheric Sciences, Oregon State University, Corvallis, OR 97331-5503.

C. Roesler, Bigelow Laboratory for Ocean Sciences, West Boothbay Harbor, ME 04575.

H. M. Sosik and A. J. Williams III, Woods Hole Oceanographic Institution, Woods Hole, MA 02543-1049.

(Received May 5, 1999; revised October 10, 2000;
accepted October 27, 2000.)